Pair-density-wave superconductor from doping Haldane chain and rung-singlet ladder

Ya-Hui Zhang [1,2] and Ashvin Vishwanath[1]
[1]*Department of Physics, Harvard University, Cambridge, Massachusetts 02138, USA*
[2]*Department of Physics and Astronomy, Johns Hopkins University, Baltimore, Maryland 21218, USA*

(Received 13 March 2022; revised 22 June 2022; accepted 24 June 2022; published 5 July 2022)

We report the numerical discovery of a Luther-Emery liquid with pair-density-wave (PDW) correlations from doping either (i) a spin-one Haldane chain or (ii) a two-leg ladder in the rung-singlet phase in which the doped charges occupy a single leg. We model these systems using a generalized Kondo model. The itinerant electrons are correlated and described by the t-J model, and are further coupled to a spin-1/2 Heisenberg model through the Kondo coupling J_K. When the density of electrons x is one, the Mott insulator is in a Haldane phase or in a rung-singlet phase depending on whether J_K is negative or positive. Upon doping, a pair-density-wave with $\mathbf{Q} = \pi$ can emerge for both signs of J_K. In the $J_K \to -\infty$ limit, the model reduces to the recently proposed type II t-J model. We also identify a composite order parameter for the superconductor, which can be understood as a Cooper pair formed by two nearby fermionic spin-polarons. Our model and the predicted PDW phase can be experimentally realized by doping $S = 1$ chains formed by Ni^{2+} in a solid-state system or a two-leg ladder of fermionic cold atoms with a potential bias between legs, which preferentially dopes carriers into a single leg. Long-range order of the PDW can be achieved in quasi-one-dimensional system with finite interwire coupling.

DOI: 10.1103/PhysRevB.106.045103

I. INTRODUCTION

The possibility of a high-T_c superconductor emerging on doping a spin-*one-half* Mott insulator has been intensively studied in the last several decades [1]. However, the fate of doping a spin-*one* Mott insulator is not well explored so far. Here we take the first steps to doping a spin-one magnet by focusing on one dimension. The one-dimensional spin-one antiferromagnet is well known to be in the Haldane phase [2–4], which is a classical example of symmetry protected topological ordered phase with edge modes [5,6]. Here however we will be interested in closing the charge gap by doping.

Various models have already been studied for doping a $S = 1$ chain. (I) In the first class of model, the $S = 1$ moment in the undoped insulator is formed by one single electron with $S = 1$ [7] or three flavors [8]. These are not realistic models of $S = 1$ in a solid-state system where the $S = 1$ is built from single electrons which carry only $S = \frac{1}{2}$. (II) In Refs. [9,10], the authors assume that the $S = 1$ moment is formed by two spin-1/2 electrons with ferromagnetic interorbital (interleg) coupling J_H. However, interorbital repulsion is ignored and a strongly bound onsite Cooper pair is formed because of this artifact. (III) References [11,12] considered two orbital model with both Hund's coupling and repulsive interaction. But there is no crystal field splitting and thus it may only be relevant to systems with additional symmetry protecting the orbital degeneracy. Such an extra symmetry is absent in a generic solid-state material where crystal field splitting is expected to be large in quasi-1D material.

In our model, the $S = 1$ moment in the undoped insulator is formed by two electrons on two orbitals coupled together by a ferromagnetic Hund's coupling J_H [13]. Then, we dope only one orbital with holes, while the other orbital is orbitally selective Mott localized [14,15] and just provides spin-1/2 local moments. Thus, we obtain a Kondo-like model, with itinerant electron in a **C** layer, which couples to $S = 1/2$ local moments in an **S** layer with a Kondo coupling $J_K = -J_H < 0$. We also discuss the case with a positive J_K, which can naturally be realized in bilayer optical lattices [16,17] with a potential difference. In the $J_K \to -\infty$ limit, the model reduces to a new kind of t-J model dubbed as type II t-J model by us in a previous paper [14]. This type II t-J model interpolates between a spin-1/2 Mott insulator and a spin one Mott insulator by tuning the density x from 0 to 1. We will report numerical discoveries of a spin gapped Luther-Emery liquid phase with pair-density-wave superconducting correlations for both signs of J_K. A PDW superconductor has Cooper pair condensed at a nonzero momentum [18] so that the effect of translation symmetry combined with a phase rotation, leaves the order parameter invariant. Similar orbital-selective Mott picture has been considered in Refs. [19,20] though the exact physics appears different from our model and a PDW phase is absent. In strictly one dimension, long-range order is forbidden. However, in real experiments one often deals with quasi-one-dimensional system with small but finite interwire correlations. In that case, full long-range order may be achieved because of interwire tunneling, given that the superconductor susceptibility diverges in our calculation without including interwire coupling.

The model with $J_K > 0$ can be realized by doping a two-leg ladder with a potential bias. Unlike previous studies which dope both legs [21], in our case only one leg is doped. We note that a PDW phase with $\mathbf{Q} = \pi$ was previously reported in a Kondo-Heisenberg model with the Heisenberg coupling

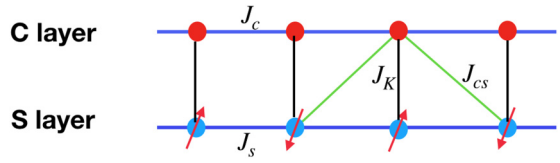

FIG. 1. Illustration of the generalized Kondo model defined in Eq. (1). The C leg hosts the correlated itinerant electrons, while the S leg corresponds to local spin-1/2 moment coming from Mott localization of another, lower energy, orbital. J_c, J_s, J_{cs} are antiferromagnetic super-exchange terms. J_K is the onsite Kondo coupling.

$J = 2t$ [22–24] and was further generalized to the case with two-dimensional array [25]. Such a model resembles our generalized Kondo model with $J_K > 0$. However, there are also some essential differences. In our model, the C layer itself is also strongly correlated and is described by a t-J model. This stabilizes the PDW phase which is now realized at a realistic parameter value of $J = 0.5t$, which could be potentially realized in two-leg ladder Fermi gas optical lattices. Recently, a cold atoms setup consisting of a bilayer optical lattice in the rung-singlet state, with an interlayer potential difference, was modeled in Refs. [26,27]. In those works, a metastable configuration is studied, in which both layers (or both legs in 1D) are doped with an equal density of charge carriers while the interlayer tunneling is assumed to be zero due to a large potential difference. In contrast, our setup considers the ground state configuration where all the holes preferentially occupy one layer. This leads to significant differences including the emergence of PDWs in our model.

II. GENERALIZED KONDO MODEL

In this paper we study a generalized Kondo model (illustrated in Fig. 1):

$$\begin{aligned} H = &-t\sum_{\langle ij\rangle;\sigma}(Pc^\dagger_{i;\sigma}c_{j;\sigma}P + \text{H.c.}) + J_c\sum_{\langle ij\rangle}\vec{S}_{i;c}\cdot\vec{S}_{j;c} \\ &+ J_s\sum_{\langle ij\rangle}\vec{S}_{i;s}\cdot\vec{S}_{j;s} + J_K\sum_i \vec{S}_{i;c}\cdot\vec{S}_{i;s} \\ &+ J_{cs}\sum_{\langle ij\rangle}(\vec{S}_{i;c}\cdot\vec{S}_{j;s} + \vec{S}_{i;s}\cdot\vec{S}_{j;c}), \end{aligned} \tag{1}$$

where J_K is a Kondo coupling. The first line is a conventional spin-1/2 t-J model with P as the projection operator to forbid double occupancy of the itinerant electron. $\vec{S}_{i;s}$ represents the local spin-1/2 moment. $\vec{S}_{i;c} = \frac{1}{2}c^\dagger_{i;\sigma}\vec{\sigma}_{\sigma\sigma'}c_{i;\sigma'}$ is the spin of the electron in the C layer. We define the density of electron to be x per site. When $x = 1$, we have an insulator which is in either a Haldane phase or in a rung-singlet phase depending on the sign of $J_K - 2J_{cs}$. We emphasize that finite super-exchange couplings J_s, J_c are important. Without them, the ground state is likely to be in a ferromagnetic phase due to the double exchange mechanism for $x < 1$ [28]. J_{cs} is not necessary but its existence will enhance the PDW phase. We will always use $t = 1, J_c = J_s = 0.5$ while varying J_K, J_{cs}, and x in our calculation.

This generalized Kondo model can be realized in either solid-state system with two orbitals ($J_K < 0$) or in bilayer optical lattice system ($J_K > 0$). We will see that a PDW superconductor phase can be found for both signs of J_K and therefore is relevant for both the solid-state realization and the bilayer optical lattice. In the following we briefly discuss how we derive the Kondo model.

A. Realization in solid-state system

We want to model a transition metal oxide with 3D electrons in atomic configuration d^{9-x}. We consider a model with two orbitals (for example, the two e_g orbitals). We use the hole picture for simplicity. A general lattice Hamiltonian is

$$\begin{aligned} H = H_K &+ \frac{U_1}{2}\sum_i n_{1;i}(n_{1;i}-1) + \frac{U_2}{2}\sum_i n_{2;i}(n_{2;i}-1) \\ &+ U'\sum_i n_{1;i}n_{2;i} - 2J_H\sum_i\left(\mathbf{S}_{1;i}\cdot\mathbf{S}_{2;i} + \frac{1}{4}n_{i;1}n_{i;2}\right), \end{aligned} \tag{2}$$

where $n_{a;i}$ is the density of the orbital a at the site i. $a = 1, 2$ denotes the $d_{3z^2-r^2}$ orbital and the $d_{x^2-y^2}$ orbital, respectively. In certain material, the energy of another orbital such as d_{xy} is lower than that of the $d_{3z^2-r^2}$ orbital in the hole picture. In this case we just use d_1 to represent the d_{xy} orbital. U_1, U_2 are intraorbital Hubbard interaction. U' is the interorbital interaction. J_H is the interorbital Hund's coupling. We assume that $U_1 = U_2 = U$ and $U - U' = 2J_H$.

The kinetic energy is

$$\begin{aligned} H_K = &-t_1\sum_{\langle ij\rangle}(d^\dagger_{1;i}d_{1;j} + \text{H.c.}) - t_2\sum_{\langle ij\rangle}(d^\dagger_{2;i}d_{2;j} + \text{H.c.}) \\ &- \sum_{\langle ij\rangle}t_{12;ij}(d^\dagger_{1;i}d_{2;j} + \text{H.c.}) + \sum_i \Delta n_{1;i}, \end{aligned} \tag{3}$$

where Δ is the crystal field splitting between the two orbitals.

We consider the limit that $\Delta \geqslant t$ but $\Delta < J_H, U', U$. We label the total density per site as $n = 1 + x$. At $x = 0$, we have one particle per site. Because of a finite Δ, there are only two possible states: $d^\dagger_{2;\uparrow}|0\rangle$ and $d^\dagger_{2;\downarrow}|0\rangle$, forming a $S = 1/2$ local moment. When $x > 0$, there are xN_s number of sites with $n = 2$, where N_s is the total number of sites. If $U - U' + J_H = 3J_H > \Delta$, then the doped particle is favored to enter the d_1 orbital to reduce repulsion and gain from Hund's coupling. In the end, d_2 orbital is always frozen and remains as spin-1/2 local moment. We then reach a Kondo-like model. If, however, $\Delta > 3J_H$, then the doped electron is favored to enter the d_2 orbital and forms a spin-singlet doublon, leading to the well-studied t-J model. In this paper we will restrict to the regime that $\Delta < 3J_H$. As shown in Appendix A, from t/U expansion we can derive the generalized Kondo model in Eq. (1) with parameters $J_c = 4\frac{t_1^2}{U}$, $J_s = 4\frac{t_2^2}{U}$, and $J_{cs} = 2\frac{t_{12}^2}{U-U'-\Delta} + 2\frac{t_{12}^2}{U+U'+\Delta}$. The Kondo coupling now is $J_K = -J_H < 0$.

$x = 1$ limit is a spin one Mott insulator with two electrons in the two orbitals forming a spin-triplet. One typical $S = 1$ Mott insulator is formed by Ni^{2+} [29] with Ni in the d^8 configuration. Therefore, we propose to realize this generalized Kondo model from doping spin-one magnet formed by Ni^{2+}. Exact parameters for each material is hard to know without a detailed study. However, we note that our model is quite generic. As long as there is a crystal field splitting between

the two orbitals, doped holes will enter only one orbital and couple to the other orbital only through the Hund's coupling.

B. Realization in bilayer optical lattice

The generalized Kondo model with $J_K > 0$ can also be naturally realized in a bilayer optical lattice system, which was recently explored in cold atom experiments [16,17]. We consider a bilayer optical lattice described by a bilayer Hubbard model:

$$\begin{aligned} H = &\Delta \sum_i n_{i;1} - t \sum_{a=1,2} \sum_{\sigma=\uparrow,\downarrow} \sum_{\langle ij\rangle} (c^\dagger_{i;a\sigma} c_{j;a\sigma} + \text{H.c.}) \\ &- t_{12} \sum_{a=1,2} \sum_{\sigma=\uparrow,\downarrow} \sum_{\langle ij\rangle} (c^\dagger_{i;1\sigma} c_{j;2\sigma} + c^\dagger_{i;2\sigma} c_{j;1\sigma} + \text{H.c.}) \\ &- t_\perp \sum_{a,\sigma} \sum_i (c^\dagger_{i;1\sigma} c_{i;2\sigma} + \text{H.c.}) - \mu \sum_{a=1,2} \sum_i n_{i;a} \\ &+ \frac{U}{2} \sum_a \sum_i n_{i;a}(n_{i;a} - 1) + U' \sum_i n_{i;1} n_{i;2}, \end{aligned} \tag{4}$$

where $n_{i;a} = \sum_\sigma c^\dagger_{i;a\sigma} c_{i;a\sigma}$ is the density at site i for layer $a = 1, 2$. $n_i = n_{i;1} + n_{i;2}$ is the total density at site i. We also define the average density $n = \frac{1}{N_s} \sum_i n_i$, where N_s is the total number of sites in the system.

The model resembles the two-orbital Hubbard model in Eq. (3), but now we have $J_H = 0$ because c_1 and c_2 are now from physically distinct layers. Here $a = 1, 2$ labels the two layers and $t_\perp$ is the interlayer vertical tunneling. A nonzero $\Delta > 0$ is caused by a displacement field, or a potential difference between the two layers. We will stay in the limit $U \gg t$ and $U \gg U'$. We assume $t_\perp, t < \Delta < U - U'$. At density $n = 1$, we have a Mott insulator with one particle at layer 2. Then at density $n = 1 + x$ with $x \in (0, 1)$, the doped additional particle enters layer 1 to reduce the onsite Hubbard U. In this case layer 2 is always Mott localized and provides a spin-1/2 moment. The itinerant electron in layer 1 is described by a t-J model which then couples to the local moment of layer 2 through a Kondo coupling. This is exactly the generalized Kondo model defined in Eq. (1) with the parameter: $J_c = J_s = \frac{4t^2}{U}, J_{cs} = 2\frac{t_{12}^2}{U-U'-\Delta} + 2\frac{t_{12}^2}{U+U'+\Delta}$, and $J_K = 2\frac{t_\perp^2}{U-U'-\Delta} + 2\frac{t_\perp^2}{U-U'+\Delta}$.

Note that we always have $J_K > 0$ because we need $\Delta < U - U'$ to make the doped particles stay in layer 1. If we increase either Δ or $t_\perp$, then we should reach a Fermi liquid phase with large Fermi surface. We will mainly focus on the regime where Δ is not large enough to destroy the layer-selective Mott localization. In this regime we can focus on the generalized Kondo model in Eq. (1) with J_K tuned by $t_\perp$ or Δ. Note in the above analysis U' is not necessary and we can set $U' = 0$. t_{12} is needed to generate a finite J_{cs}, which is not necessary, but can enhance the PDW phase.

The $x = 1$ limit is a bilayer Mott insulator with a spin-1/2 moment at each layer for each site i. When $x < 1$, we dope finite density of holes into layer 1 because of the potential difference Δ, while layer 2 remains Mott localized. If there is no interlayer coupling, then layer 1 is clearly described by the conventional t-J model. In our case, this t-J model further couples to another spin-1/2 model through a Kondo coupling J_K.

III. PDW SUPERCONDUCTOR

We study the generalized Kondo model in Eq. (1) using density matrix renormalization group (DMRG) method [30,31]. We use both the finite size DMRG and the infinite DMRG (iDMRG) [32]. They give consistent results but have their own advantages on different tasks. Finite DMRG is more convenient to tune the doping x with a small step. Typical system size L_x is 100 in our calculation, but we also have results with $L_x = 80, 100, 120$ to do $\frac{1}{L_x}$ scaling. The infinite DMRG is more useful to extract central charge and fit the power-law exponent without worrying about boundary effects. In our problem, we want a doping x larger than 0.9. Then we need a large unit cell size. We typically use a unit cell size $L = 30$ and put 28 electrons within each unit cell to get $x = \frac{28}{30} \approx 0.93$. This unit cell is repeated for infinitely long in the iDMRG algorithm. Translation invariance within the unit cell is not enforced by the algorithm but will be reached in the end by minimizing the energy. Both the finite DMRG and iDMRG simulations are performed using the TeNPy Library (version 0.4.0) [33]. For infinite DMRG, we use unit cell size $L = 30$ and bond dimension up to $m = 2000$, which gives a typical truncation error at order 10^{-5}. The convergence with the bond dimension is demonstrated below. In iDMRG it is also convenient to extract correlation lengths for various different operators using the transfer matrix method [33]. Such data with different bond dimensions $m = 500, 1000, 2000$ can be found in Appendix C. For finite DMRG with system size $L_x \sim 100$, we use bond dimension up to $m = 2000$, which can achieve truncation error at order 10^{-6}. The convergence with the bond dimension and the $1/L_x$ scaling is shown in Appendix C.

In Fig. 2 we show evidences for a Luther-Emery liquid with quasi-long-range PDW order parameter. In Fig. 2(a) we show a finite spin gap Δ_S when $J_K \in (-\infty, J_K^c)$. In our DMRG simulation the spin S_z is conserved. The ground state is found in the $S_z = 0$ sector and the spin gap is defined as $\Delta_S = E(S_z = 1) - E(S_z = 0)$ (see more details in Appendix B). We note that a nonzero J_{cs} can enhance the spin gap [see Fig. 2(b)]. When $J_K > J_K^c$ ($J_K^c \approx 0.95$ for $J_{cs} = 0.25$), the ground state is in a Luttinger liquid phase with zero spin gap. Inside the spin gap phase, there is power-law decay for the correlation function of the spin-singlet pairing order parameter defined as $P(x) = \epsilon_{\sigma\sigma'} c_\sigma(x) c_{\sigma'}(x+1)$, where $\epsilon_{\sigma\sigma'}$ is the Levi-Civita symbol. We find that $\langle P^\dagger(x) P(0)\rangle \sim (-1)^x \frac{1}{x^{K_{sc}}}$, shown in Fig. 2(c). The oscillations $(-1)^x$ implies that the order parameter has a momentum $\mathbf{Q} = \pi$, hence the phase is a PDW superconductor. The power-law decay is demonstrated in Fig. 3(a). We extract K_{sc} from a linear fit. We also obtain the Luttinger parameter K_c using the method discussed in Appendix B. As shown in Fig. 3(b), we find $K_c \approx K_{sc}^{-1}$ as expected for a Luther-Emery liquid. K_c can be larger than 1, indicating slower decay of the superconductor (SC) order than the charge-density-wave (CDW) order. However, when varying J_K at fixed $J_{cs} = 0.25$, K_c has a dip at $J_K^0 \approx 0.45$, which separates the PDW phase into two domes. It is known that the susceptibility of the superconducting order

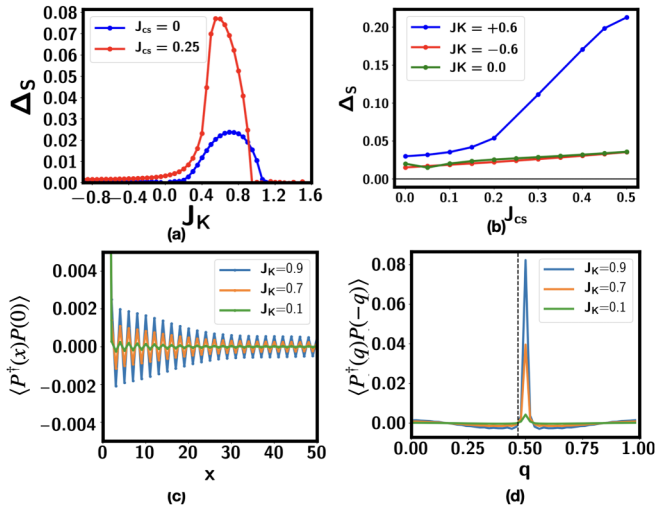

FIG. 2. Evidence for PDW phase in the generalized Kondo model defined in Eq. (1). (a) Spin gap $\Delta_S(L_x=\infty)$ as a function of J_K for $J_{cs}=0,\ 0.25$ at the doping $x=0.9$ in units of $t=1$. The value is obtained from extrapolation of finite size results with $L_x=80, 100, 120$. There is still a finite spin gap in the negative J_K regime if one zooms in (see Fig. 9 in Appendix C). The spin gap closes at $J_K^c\approx 1.05,\ 0.95$ for $J_{cs}=0,\ 0.25$. (b) Spin gap as function of J_{cs} at $x=0.96$ using system size $L_x=100$ for fixed $J_K=-0.6, 0, +0.6$. (c) Pairing-pairing correlation function in real space from infinite DMRG. We use $J_{cs}=0.25$ and $x=\frac{28}{30}\approx 0.933$ with unit cell size $L=30$. Here $P(x)=\epsilon_{\sigma\sigma'}c_\sigma(x)c_{\sigma'}(x+1)$ is the spin-singlet Cooper pair on a nearest-neighbor bond, where $\epsilon_{\sigma\sigma'}$ is the Levi-Civita symbol. (d) The Fourier transformation of the pairing-pairing correlation, peaked at $q=\pi$. Here q is in unit of 2π and the dashed line labels $2k_F=\frac{x}{2}\times 2\pi$.

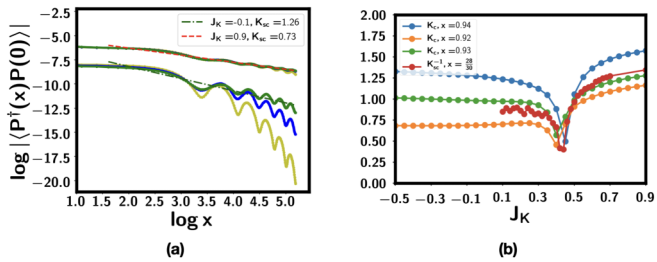

FIG. 3. (a) Log-Log plot of the pairing correlation function and distance x at $J_{cs}=0.25$ for $J_K=-0.1$ and $J_K=0.9$. We use infinite DMRG with unit cell size $L=30$ and the density is at $x=\frac{28}{30}$. The top three lines are for $J_K=0.9$ and the bottom three lines are for $J_K=-0.1$. Within each group, we plot the results for $m=500, 1000, 2000$ with color yellow, blue and green. For $J_K=0.9$, there is almost no difference for different bond dimensions. For $J_K=-0.1$, the pairing correlation function is an exponential decay, but the correlation length increases with bond dimension m and the log-log plot moves towards a straight line when increasing m. The green and red dashed lines are the linear fit for $J_K=-0.1$ and $J_K=0.9$, respectively. (b) The inverse of the power-law decay exponent for the pairing correlation function K_{sc}^{-1} and the Luttinger parameter K_c as a function of J_K. We used $J_{cs}=0.25$. K_{sc} is fit from infinite DMRG results shown in (a). K_c is fit from finite DMRG results at several fillings at size $L_x=100$. We find $K_{sc}^{-1}\approx K_c$ evaluated at $x=0.93$. Luttinger parameter K_c has a dip at $J_K=J_K^0\approx 0.45$, separating the PDW phase into two domes.

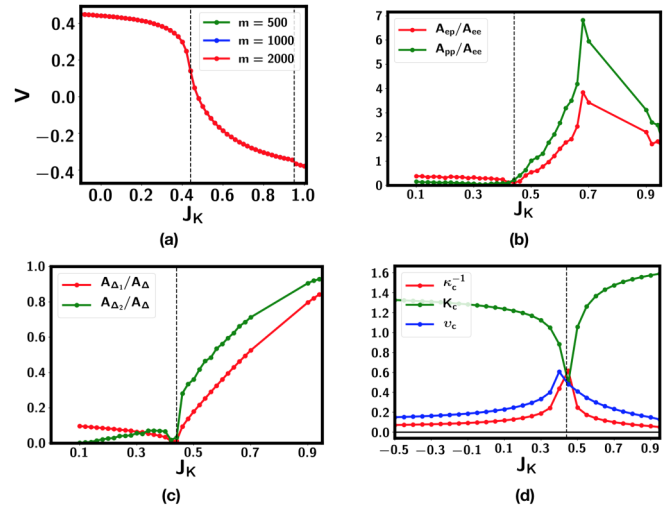

FIG. 4. Evolution with J_K at fixed $J_{cs}=0.25$. (a) Rung spin-correlator $V=\langle\vec{S}_{i;c}\cdot\vec{S}_{i;s}\rangle+\frac{1}{4}$ from infinite DMRG at $x=\frac{28}{30}\approx 0.933$ with a unit cell size of $L=30$. The two dashed lines are at $J_K^0=0.44$ and $J_K^c=0.95$. Here m is the bond dimension. (b) Amplitudes for Green functions of electron or polaron. The vertical dashed line is at $J_K^0=0.44$. (c) Amplitudes for pairing-pairing correlation of composite Cooper pairs. The vertical dashed line is at $J_K^0=0.44$, on either side of which the composite operator amplitudes grow. The same parameters are used as in panels (a, b). (d) Inverse charge compressibility κ_c^{-1}, Luttinger parameter K_c, Fermi velocity of the charge mode υ_c at $x=0.94$ from finite DMRG with system size $L_x=100$. We have used $\kappa_c=\frac{\pi}{2}\frac{K_c}{\upsilon_c}$ to extrapolate υ_c. The vertical dashed line is at $J_K^0=0.45$, which separates the two PDW domes.

parameter χ diverges at low temperature with a relation $\chi(T)\sim T^{-(2-K_{SC})}$ [21]. Therefore, when the temperature approaches zero, superconductivity susceptibility has a strong divergence in our model given that $K_{SC}<2$. Thus, long-range order may be achieved if one considers a quasi-1D system and includes a fintie interwire coupling.

It turns out the interleg spin-spin correlation changes from ferromagnetic to antiferromagnetic precisely at J_K^0, which is defined as the dip of K_c as shown in Fig. 3(b). We define a rung spin-correlator $V_i=\langle\vec{S}_{i;c}\cdot\vec{S}_i\rangle+\frac{1}{4}$ to characterize the interleg spin-spin correlation. V changes sign around J_K^0, as shown in Fig. 4(a). As shown in Appendix C, there is a rapid crossover but no phase transition, at J_K^0. At $J_K^c\approx 0.95$, there is a small jump of V, suggesting a first order transition between the PDW phase and the Luttinger liquid phase with zero spin gap.

We also point out the existence of spin-polarons at low energy when moving away from J_K^0 toward both sides. The spin-polaron is a bound state of electron in the C layer and spin operator in the S layer:

$$\tilde{c}_{i;\sigma}=\tfrac{1}{2}(\vec{S}_{i;s}\cdot\vec{\sigma}_{\sigma\sigma'})c_{i;\sigma'},\tag{5}$$

where $\vec{\sigma}$ is the Pauli matrix and $\vec{S}$ is the spin operator of the S layer. This composite operator $\tilde{c}_\sigma$ has the same quantum number as the microscopic electron operator c_σ.

It can be easily shown that $c_{i;\sigma}^\dagger\tilde{c}_{i;\sigma}=\vec{S}_{i;c}\cdot\vec{S}_{i;s}$. Thus, for either sign of $\langle\vec{S}_{i;c}\cdot\vec{S}_{i;s}\rangle$, there is a hybridization between the electron and the spin polaron. To characterize

this hybridization, we define several different equal-time Green functions: the single electron Green function $G_{\sigma;ee}(x,y) = \langle c^\dagger_\sigma(x) c_\sigma(y)\rangle$; electron-polaron Green function $G_{\sigma;ep}(x,y) = \langle c^\dagger_\sigma(x)\tilde{c}_\sigma(y)\rangle_c$ and polaron-polaron Green function $G_{\sigma;pp}(x,y) = \langle \tilde{c}^\dagger_\sigma(x)\tilde{c}_\sigma(y)\rangle_c$. Here we have subtracted the average values so that $G_{\sigma;ep}(x,y) = G_{\sigma;pp}(x,y) = 0$ in the decoupled limit $J_K = J_{cs} = 0$. For each type $\alpha = ee, ep, pp$, we find that $G_{\sigma;\alpha}(x,0) = A_\alpha e^{-\frac{x}{\xi}}$ in the PDW phase with the same exponent ξ. In Fig. 4(b), we show that $\frac{A_{ep}}{A_{ee}}$, $\frac{A_{pp}}{A_{ee}}$ vanish at J_K^0. Across J_K^0, the interlayer spin-spin correlation changes sign and the mixture between the polaron and the electron vanishes. This coincides with the dip of K_c, strongly suggesting that the existence of polaron is crucial for a large K_c, presumably from effective attractive interaction. Especially in the $J_K^0 < J_K < J_K^c$ regime, the ratio of amplitudes $\frac{A_{pp}}{A_{ee}} \gg 1$, indicating dominance of the polaron at low energy. This is also the regime where the PDW superconductor is strongest and the decay of the pairing correlation is the slowest.

With the spin-polaron, we can also define the composite Cooper pair of an electron and a polaron, or a Cooper pair of two polarons. We can define the usual spin-singlet Cooper pair $\Delta(x) = \epsilon_{\sigma\sigma'} c_\sigma(x) c_{\sigma'}(x+1)$ and two composite Cooper pairs: $\Delta_1(x) = \frac{1}{3}\{\vec{\Delta}_T(x)\cdot[\vec{S}_s(x) - \vec{S}_s(x+1)]\}$ and $\Delta_2(x) = \Delta(x)\vec{S}_s(x)\cdot\vec{S}_s(x+1)$. In the above $\vec{\Delta}_T(x)$ is the spin-triplet Cooper pair on the nearest-neighbor bond and $\vec{S}_s(x)$ is the spin operator in the S layer. In Appendix D 2 we show that Δ_1 is the Cooper pair between electron and polaron while Δ_2 is from the Cooper pair of two polarons. We expect the existence of all these three Cooper pairs at low energy. Indeed we find that $\langle \Delta^\dagger_\alpha(x)\Delta_\alpha(0) = A_\alpha \frac{(-1)^x}{x^{K_{SC}}}$ for $\alpha = \Delta, \Delta_1, \Delta_2$ with the same exponent K_{sc}. Again $\frac{A_{\Delta_1}}{A_\Delta}$ and $\frac{A_{\Delta_2}}{A_\Delta}$ vanish at J_K^0 as shown in Fig. 4(c), confirming the absence of the polaron here. In the regime $J_K^0 < J_K < J_K^c$, the amplitude for the polaron-polaron Cooper pair is the strongest. This again highlights the importance of the polaron for the PDW superconductor.

In summary, at J_K^0, the mixture of the polaron and the electron is the weakest because the interlayer spin-spin correlation vanishes. Moving away from J_K^0 to either the ferromagnetic and antiferromagnetic side, there is a hybridization between electron and polaron. In the same time, the Fermi velocity decreases and the Luttinger parameter increases [see Fig. 4(d)], indicating effective attractive interactions. One simple explanation is that now the spin-spin exchange between the spin polarons has contributions from J_c, J_s, J_{cs}, which add up to induce a strong attraction between two nearby polarons.

IV. BOSONIZATION ANALYSIS

The existence of the PDW phase can be understood from a bosonization analysis starting from the decoupled limit with $J_{cs} = J_K = 0$ following Refs. [22,34]. At the decoupled limit we have one charge and one spin mode from the C layer and an additional spin mode from the S layer. We can label the bosonization variables of the charge mode as θ_c, ϕ_c, of the spin mode of the C layer as θ_s, ϕ_s and of the spin mode in the S layer as $\tilde{\theta}_s, \tilde{\phi}_s$. With the inclusion of J_K, J_{cs}, the two spin modes mix with each other and we can define new variable $\theta_{s;\pm} = \frac{1}{\sqrt{2}}(\theta_s \pm \tilde{\theta}_s)$ and $\phi_{s;\pm} = \frac{1}{\sqrt{2}}(\phi_s \pm \tilde{\phi}_s)$. It can be shown that the most relevant interlayer coupling term gives $-g\cos 2\theta_{s;-}\cos 2\phi_{s;+}$. In Appendix G we show that this term is relevant when $J_K + 2J_{cs} > 0$ in the weak coupling limit. Therefore, when $J_K + 2J_{cs} > 0$, this term pins $\theta_{s;-} = 0\,(\pi)$ and $\phi_{s;+} = 0\,(\pi)$ and the two spin modes are gapped. We are left with only the charge mode, leading to a spin gapped Luther-Emery liquid phase with algebraic superconductor (SC) and CDW order.

However, correlation functions for simple $Q = 0$ SC order defined in the C layer are exponentially decaying. We have spin-singlet SC order $\Delta_S \sim e^{i\sqrt{2}\theta_c}\cos\sqrt{2}\phi_s$ and spin-triplet SC order $\Delta_T \sim e^{i\sqrt{2}\theta_c}(\sin\sqrt{2}\theta_s, \cos\sqrt{2}\theta_s, \sin\sqrt{2}\phi_s)$. We note that $\phi_s = \frac{1}{\sqrt{2}}(\phi_{s;+} + \phi_{s;-})$ is always fluctuating because $\theta_{s;-}$ is pinned. Similarly θ_s is fluctuating because $\phi_{s;+}$ is ordered and all of these order parameters are gapped. To get algebraic decay, we need a composite order parameter by attaching an operator in the S layer. First, in S layer we can define Neel order parameter $(n_x, n_y, n_z) \sim (\sin\sqrt{2}\tilde{\theta}_s, \cos\sqrt{2}\tilde{\theta}_s, \sin\sqrt{2}\tilde{\phi}_s)$. Meanwhile, there is a VBS order parameter $\tilde{V} \sim \cos\sqrt{2}\tilde{\phi}_s$. The Neel and VBS order parameters carry momentum $\mathbf{Q} = \pi$. Now we can define a composite order parameter $O_{\mathrm{PDW}} \sim \Delta_S\tilde{V} \sim \vec{\Delta}_T\cdot\vec{n} \sim e^{-i\sqrt{2}\theta_c}$ which carries momentum $\mathbf{Q} = \pi$ and is a spin-singlet. We have $O_{\mathrm{PDW}}(x)O_{\mathrm{PDW}}(0) \sim \frac{1}{x^{K_c}}$. Note that these composite order parameters $\Delta_S\tilde{V}$ and $\vec{\Delta}_T\cdot\vec{n}$, combined with a factor $(-1)^x$, are precisely Δ_1 and Δ_2 defined previously from electron-polaron Cooper pair and polaron-polaron Cooper pair.

V. TYPE II *t-J* MODEL

Although a PDW phase at $J_K > 0$ side can be explained by bosonization, at least in the small J_K limit, its existence at $J_K < 0$ side is a surprise. In this subsection we show the existence of a PDW phase even at the $J_K \to -\infty$ limit. In the $J_K \to -\infty$ limit, we can obtain a type II t-J model which was recently proposed by us [14]. The model has two spin-1/2 singlon states (defined as states with $\sum_\sigma c^\dagger_{i;\sigma}c_{i;\sigma} = 0$) and three $S = 1$ doublon states(defined as states with $\sum_\sigma c^\dagger_{i;\sigma}c_{i;\sigma} = 1$) at each site. Here singlon is defined as singly occupied site and the doublon is defined as the doubly occupied site. The model can be written as

$$H = -t\sum_{\langle ij\rangle;\sigma}(Pc^\dagger_{i;\sigma}c_{j;\sigma}P + \mathrm{H.c.}) + J_s\sum_{\langle ij\rangle}\vec{s}_i\cdot\vec{s}_j + J_d\sum_{\langle ij\rangle}\vec{S}_i\cdot\vec{S}_j + J_{sd}\sum_{\langle ij\rangle}(\vec{s}_i\cdot\vec{S}_j + \vec{S}_i\cdot\vec{s}_j), \quad (6)$$

where $\vec{s}$ is the spin operator of the singlon with $S = \frac{1}{2}$ and $\vec{S}$ is the spin operator of the doublon with $S = 1$. The c operator is the electron operator in Eq. (1) projected to the restricted Hilbert space forbidding the $S = 0$ doublon. Now the projection operator P restricts to a five-dimensional Hilbert space at each site i: two singlon states and three doublon states. Note that the original Kondo model in Eq. (1) has six states at each site. Here we remove the $S = 0$ doublon state, meaning the electron in C layer and the spin in the S layer forms a spin singlet. We have $J_s = J_s$, $J_d = \frac{1}{2\sqrt{2}}(J_c + J_s + 2J_{cs})$, and $J_{sd} = \frac{1}{2}(J_s + J_{cs})$. This model should be the effective t-J

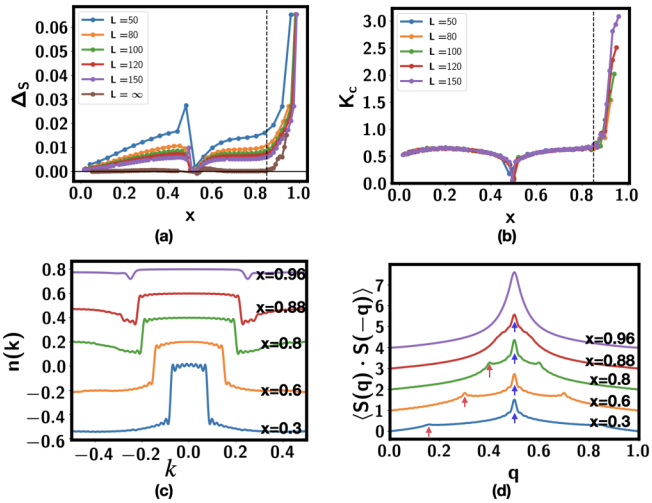

FIG. 5. Evolution with doping x in the type II t-J model with doping x, setting $t = 1, J_s = J_d = 0.5, J_{sd} = 0.25$. The momentum in the plot is in units of 2π. (a) Spin gap Δ_S with x. Δ_S at $L = \infty$ is extrapolated from that of the finite L. The dashed line is at $x_c = 0.85$, which denotes the onset of a finite spin gap. (b) Luttinger parameter K_c with x. (c) Momentum distribution function $n(k) = \langle c^\dagger_\sigma(k)c_\sigma(k)\rangle$. Curves for different x are displaced so the absolute value is not meaningful. One can see a small pocket with $k_F = \frac{x}{4}2\pi$ when $x < x_c$. (d) Spin-spin structure factor. Characteristic of LL*, there are two modes at momentum $2k_F$ and π when $x < x_c$, denoted by red arrows and blue arrows, respectively.

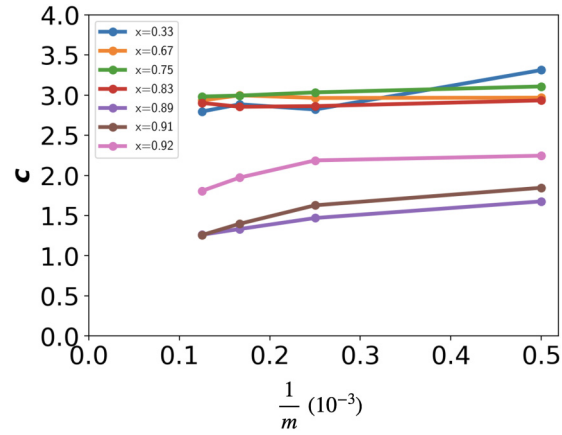

FIG. 6. Central charge at different doping x in the type II t-J model, using the same parameter as in Fig. 5. The central charge is fit from the relation $S = \frac{c}{6}\log\xi$ in infinite DMRG, where S is the entanglement entropy and ξ is the correlation length. Both S and ξ grow with the bond dimension D, therefore $c = 6\frac{\delta S}{\delta\xi}$ also changes with bond dimension m. We plot c with the bond dimension m by varying m from 2000 to 8000. For $x < 0.85$, we find $c \approx 3$ in the whole range of m, consistent with a LL* phase with one charge mode and two spin modes. For $x > 0.85$, the central charge is smaller and decreases as m increases. We believe c will flow to 1 in the $\frac{1}{m} \to 0$ limit.

model from doping a $S = 1$ Mott insulator with large Hund's coupling and crystal field splitting. On average, the N_s atoms in the chain are each in the d^{9-x} state, or equivalently, there are $(1-x)N_s$ number of $S = \frac{1}{2}$ sites in the d^9 configuration and xN_s number of S=1 sites in the d^8 configuration.

While the rest of this paper has focused on doping close to unity, here a wider range of doping is displayed and the emergence of an unusual Luttinger liquid with small Luttinger volume is pointed out. In Fig. 5 we show results for the type II t-J model. We find a phase transition between a fractional Luttinger liquid (LL*) phase [15,35] ($x < x_c$) and the PDW superconductor ($x > x_c$) at around $x_c = 0.85$. At $x = 0.5$ a charge-density-wave (CDW) insulator is obtained. The LL* phase has one spinful small Fermi surface with volume $2k_F = \frac{x}{2}2\pi$ and an additional spin mode at momentum π (for details, see Ref. [15]). It can be labeled as C1S2, meaning one charge mode and two spin modes. The onset of the spin gap at x_c is shown in Fig. 5(a). When $x > x_c$, the ground state is in a Luther-Emery liquid with only one charge mode and can belabeled as C1S0. Meanwhile the Luttinger parameter K_c becomes large when $x > x_c$ shown in Fig. 5(b), giving slow decay of pair-pair correlation function. The pair correlation function again reveals the oscillatory behavior of a PDW (see Appendix F). Thus, again we see that a lightly doped Haldane chain in this large Hund's coupling limit, also reveals PDW superconductivity.

A key observation is that the LL* phase is qualitatively similar to the phase in the decoupled limit of the generalized Kondo model, although now we actually have $J_K = -\infty$. In the $J_K = -\infty$ limit, we can remove J_K by dealing with the type II t-J model with a restricted Hilbert space. It can be shown [15] that there are emergent orbitals which form effective $\tilde{C}$ layer and $\tilde{S}$ layer. In terms of the $\tilde{C}$ and $\tilde{S}$ layer, there is no Hund's coupling $-J_K$ anymore, as such a term does not exist in the type II t-J model. There can be effective antiferromagnetic spin-spin coupling between the $\tilde{C}$ and the $\tilde{S}$ layers coming from $J_s, J_d, J_{sd} > 0$ terms in the type II t-J model. Such a coupling resembles an antiferromagnetic J_{cs} coupling in terms of the new emergent orbitals and can drive the LL* phase into a PDW phase following the same bosonization analysis as in the weak coupling limit of the generalized Kondo model. In Fig. 6 we also show that the central charge jumps from $c = 3$ to $c = 1$ across this transition, which is expected for a transition between C1S2 phase and C1S0 phase.

VI. CONCLUSION

In summary, using a combination of numerical calculations and analytical arguments, we predict PDW superconductor on doping a spin-one Haldane chain or the rung-singlet phase in a two leg ladder. Experimentally, the former may be realized by doping a spin-one chain formed by Ni^{2+} [29], while the latter can be realized by a two-leg ladder of fermionic atoms in an optical lattice, by preferentially doping one of the legs. We show that the formation of a fermionic spin polaron is crucial for a robust PDW phase with slow decay of pairing correlation. Note, although we are here doping the Haldane chain, a paradigmatic example of an symmetry protected topological (SPT) phase, the edge modes have not played any role. It is left to future work if SPT physics has any role to play, given the presence of low energy charge excitations [36,37]. The models studied here can be defined in any dimension, so the

extension to two dimensions for instance should throw light on the intrinsic mechanism leading to PDWs and the role of spin-polarons in mediating pairing in strongly correlated systems. Recently Haldane chain was also realized in organic material [38,39]. It is interesting to generalize our model to such case.

ACKNOWLEDGMENTS

We thank A. Bohrdt, R. Verresen, and E. Khalaf for discussions. Support from Simons Collaboration on Ultra Quantum Matter, a grant from the Simons Foundation (Grant No. 651440, A.V.), and a Simons Investigator award are acknowledged.

APPENDIX A: GENERALIZED KONDO MODEL AND TYPE II *t-J* MODEL IN SOLID-STATE SYSTEM

1. Generalized Kondo model

We start from the two-orbital Hubbard model in Eqs. (2) and (3). We restrict to the regime that $\Delta < U - U' + J_H = 3J_H$ (we assume $U - U' = 2J_H$), then at total density $n = 1 + x$, we have itinerant particles from the d_2 orbital, while the d_1 orbital is Mott localized.

If $\Delta < 3J_H$, then the doped hole starting from the d^9 state will only enter the d_1 orbital while the d_2 orbital is always singly occupied. In another word, the d_2 orbital is orbitally selective Mott localized. Then we are left with a Kondo-like model where a conventional t-J model coupled to spin-1/2 local moment. We assume $U, U' \gg t$, so the itinerant electron in the d_1 orbital itself is strongly correlated and is described by a t-J model, which then couples to the local spin-1/2 moment from the d_2 orbital. We then define $c_{i;\sigma} = P d_{i;1\sigma} P$, where P is the projection operator to remove the double occupancy. Then we reach a Kondo-like model:

$$\begin{aligned} H = & -t \sum_{\langle ij \rangle} (c_i^\dagger c_j + \text{H.c.}) + J_c \sum_{\langle ij \rangle} \vec{S}_{i;c} \cdot \vec{S}_{j;c} \\ & + J_s \sum_{\langle ij \rangle} \vec{S}_{i;s} \cdot \vec{S}_{j;s} + J_K \sum_i \vec{S}_{i;c} \cdot \vec{S}_{i;s} \\ & + J_{cs} \sum_{\langle ij \rangle} (\vec{S}_{i;c} \cdot \vec{S}_{j;s} + \vec{S}_{i;s} \cdot \vec{S}_{j;c}), \end{aligned} \tag{A1}$$

where $J_K = -J_H$ is the ferromagnetic onsite Hund's coupling. The first two terms are the conventional spin-1/2 t-J model. The third term is the Heisenberg model of the spin-1/2 localized spin. The last line is the spin-spin coupling between the itinerant electron and the localized spin. J_c is the super-exchange term between the itinerant electron. J_s is the super-exchange between the localized spins. J_{cs} is the super-exchange between the itinerant electron and the localized spin.

The spin-spin coupling parameters can be derived from second order perturbation theory as

$$\begin{aligned} & J_c = 4\frac{t_1^2}{U}, \quad J_s = 4\frac{t_2^2}{U}, \\ & J_{cs} = 2\frac{t_{12}^2}{U - U' - \Delta} + 2\frac{t_{12}^2}{U + U' + \Delta}, \\ & J_K = -J_H, \end{aligned} \tag{A2}$$

which is derived by assuming J_H is small compared to U', U.

In principle we should also include some three-site correlated hopping processes from t^2/U. We will ignore them following the same procedure in the usual t-J model. They are listed below as

$$\begin{aligned} H' = & -\frac{J_c}{4} \sum_i (c_{i+1;\sigma}^\dagger c_{i-1;\sigma} n_{i;\bar{\sigma}} - c_{i+1;\uparrow}^\dagger c_{i;\downarrow} S_{i;c}^- - c_{i+1;\downarrow}^\dagger c_{i;\uparrow} S_{i;c}^+) + \text{H.c.} \\ & - \sum_{ij} \left[\left(\frac{2t_{12}^2}{U - U' - \Delta} - \frac{2t_{12}^2}{U - \Delta} \right) - \left(2\frac{t_{12}^2}{U + \Delta} - \frac{2t_{12}^2}{U + \Delta + U'} \right) \right] n_j \vec{S}_{i;c} \cdot \vec{S}_{j;s} \\ & + \sum_{\langle ij \rangle} \left[-\frac{t_1^2}{U} + \left(\frac{t_{12}^2}{U - U' - \Delta} - \frac{t_{12}^2}{U - \Delta} \right) - \left(\frac{t_{12}^2}{U + \Delta} - \frac{t_{12}^2}{U + \Delta + U'} \right) \right] n_i n_j \\ & + \frac{1}{2} \sum_i (c_{i+1;\sigma}^\dagger c_{i-1;\sigma}) \left[\left(\frac{t_{12}^2}{U' + \Delta} - \frac{t_{12}^2}{U - U' - \Delta} \right) + \left(\frac{t_{12}^2}{\Delta} - \frac{t_{12}^2}{U' + \Delta} + \frac{t_{12}^2}{U - U' - \Delta} - \frac{t_{12}^2}{U - \Delta} \right) n_i \right] \\ & + \sum_i (c_{i+1;\sigma}^\dagger \vec{\sigma}_{\sigma\sigma'} c_{i-1;\sigma'}) \cdot \vec{S}_i \left[\left(\frac{t_{12}^2}{U' + \Delta} + \frac{t_{12}^2}{U - U' - \Delta} \right) + \left(\frac{t_{12}^2}{\Delta} - \frac{t_{12}^2}{U' + \Delta} - \frac{t_{12}^2}{U - U' - \Delta} + \frac{t_{12}^2}{U - \Delta} \right) n_i \right]. \end{aligned} \tag{A3}$$

In the above we have hidden the projection operator to impose the constraint that there is no double occupancy in the C layer.

2. Type II *t-J* model

The type I and type II t-J model can be reached by taking $J_K \to +\infty$ limit and $J_K \to -\infty$ limit, respectively, from the generalized Kondo model. Let us take the $J_K \to -\infty$ limit, then we need to remove the interorbital spin singlet from the Hilbert space and get the type II t-J model [14,15] with two spin-1/2 singlon and three $S = 1$ doublon at each site. Here singlon is defined as singly occupied site and the doublon is defined as the doubly occupied site. The model can be written as

$$\begin{aligned} H = & -t \sum_{\langle ij \rangle} (c_i^\dagger c_j + \text{H.c.}) + J_s \sum_{\langle ij \rangle} \vec{s}_i \cdot \vec{s}_j + J_d \sum_{\langle ij \rangle} \vec{S}_i \cdot \vec{S}_j \\ & + J_{sd} \sum_{\langle ij \rangle} (\vec{s}_i \cdot \vec{S}_j + \vec{S}_i \cdot \vec{s}_j), \end{aligned}$$

where $\vec{s}$ is the spin operator of the singlon with $S = \frac{1}{2}$ and $\vec{S}$ is the spin operator of the doublon with $S = 1$. c is the electron operator in the Kondo model projected to the restricted Hilbert space with spin-1/2 singlon and $S = 1$ doublon. We have

$$J_s = J_s, \quad J_d = \frac{1}{2\sqrt{2}}(J_c + J_s + 2J_{cs}),$$
$$J_{sd} = \frac{1}{2}(J_s + J_{cs}). \tag{A4}$$

APPENDIX B: EXTRACTION OF LUTTINGER PARAMETER AND COMPRESSIBILITY IN DMRG

We use the following formula to extract the Luttinger parameter K_c for the charge mode:

$$N(\mathbf{q}) = \langle n(\mathbf{q})n(-\mathbf{q})\rangle = N(\mathbf{q}=0) + \frac{K_\rho}{\pi}q \tag{B1}$$

when $q \to 0$.

Here, we do the Fourier transformation of

$$\langle n(\mathbf{x})n(0)\rangle = -\frac{K_\rho}{\pi^2}\frac{1}{x^2} \tag{B2}$$

to get

$$N(\mathbf{q}) = \sum_{\mathbf{x}=0}^{L}\langle n(\mathbf{x})n(0)\rangle. \tag{B3}$$

We also try to extract the charge compressibility κ_c. It is known that

$$\frac{1}{\kappa_c} = \frac{\partial\mu}{\partial n} = \frac{\partial^2 E}{\partial n^2} = \frac{1}{L}\frac{E(n+\delta n) + E(n-\delta n) - 2E(n)}{\delta n^2}. \tag{B4}$$

Similarly, there is a spin compressibility κ_s extracted from

$$\frac{1}{\kappa_s} = \frac{\partial^2 E}{\partial S_z^2} = \frac{1}{L}\frac{E(S_z=1) + E(S_z=-1) - 2E(S_z=0)}{\left(\frac{1}{2}/L\right)^2}$$
$$= 8\Delta_S L, \tag{B5}$$

where $\Delta_S = E(S_z=1) - E(S_z=0)$.

In Luttinger liquid theory, it is known that

$$\kappa_c = \frac{2K_c}{\pi v_c}. \tag{B6}$$

APPENDIX C: MORE RESULTS ON THE GENERALIZED KONDO MODEL

1. Pairing correlation in real space and momentum space

In Fig. 7 we show the comparison of pair-pair correlation function obtained from finite and infinite DMRG. In finite DMRG, we see that the pair-pair correlation function has a sharp drop at the boundary of the system. This turns out to enhance a peak in the fourier transform at momentum $q = 2k_F = \frac{x}{2}\times 2\pi = \frac{48}{100}\times 2\pi$. We note that the $2k_F$ part in the pair-pair correlation function should have a large decay exponent $K_c + \frac{1}{K_c} > 2$ and should be much smaller than the peak at $q = \pi$. Indeed, in infinite DMRG, we find the feature at $q = 2k_F$ is significantly weaker because there is no boundary effect.

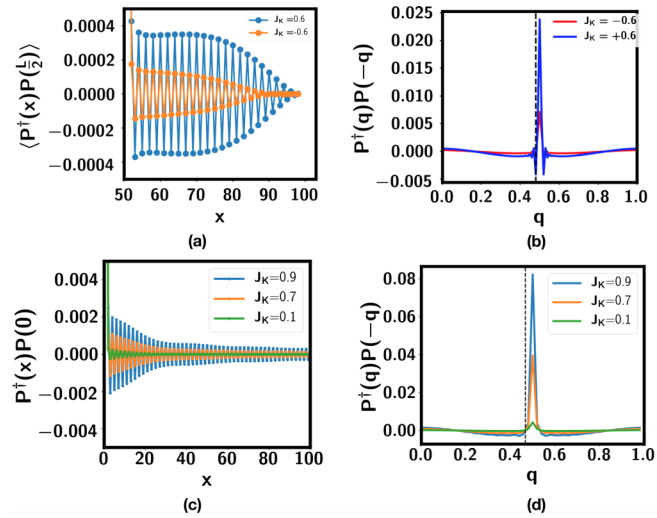

FIG. 7. We show pair-pair correlation function for $J_{cs} = 0.25$ from finite DMRG and infinite DMRG. (a, b) Pair-pair correlation function in real and momentum space from finite DMRG. $x = 0.96$ with system size $L_x = 100$. (c, d) Pair-pair correlation function in real and momentum space from infinite DMRG with unit cell size $L = 30$ and $x = \frac{28}{30}$. The vertical dashed lines are at $q = 2k_F = \frac{x}{2}\times 2\pi$. In the Fourier transformation of $P^\dagger(x)P(0)$, we ignored the short distance contribution with $|x| = 0, 1$.

2. Spin gap and spin correlation length

We report more results on spin gap from finite DMRG calculation of the generalized Kondo model. We always use $t = 1, J_c = J_s = 0.5$. We will vary J_K, J_{cs}, and the doping x. First, we show that the spin gap and our calculation converges when increasing the bond dimension from $m = 500$ to $m = 2000$, shown in Fig. 8. With bond dimension $m = 2000$, we find that the truncation error is smaller than 10^{-7} inside the PDW phase and the energy convergence (difference between $m = 1000$ and $m = 2000$) is smaller than 10^{-6}. We will use $m = 2000$ in the remaining plots.

In Fig. 9 we show how we extract the spin gap at $L = \infty$ from the results at finite $L = 80, 100, 120$. One can see a finite spin gap when $J_K < J_K^c$, where $J_K^c = 1.05, 0.95$ for

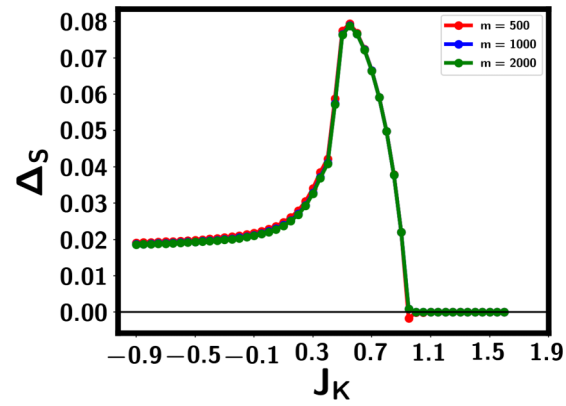

FIG. 8. Spin gap from finite DMRG with bond dimension $m = 500, 1000, 2000$. We use $x = 0.94$ with system size $L_x = 100$. We use $t = 1, J_c = J_s = 0.5, J_{cs} = 0.25$.

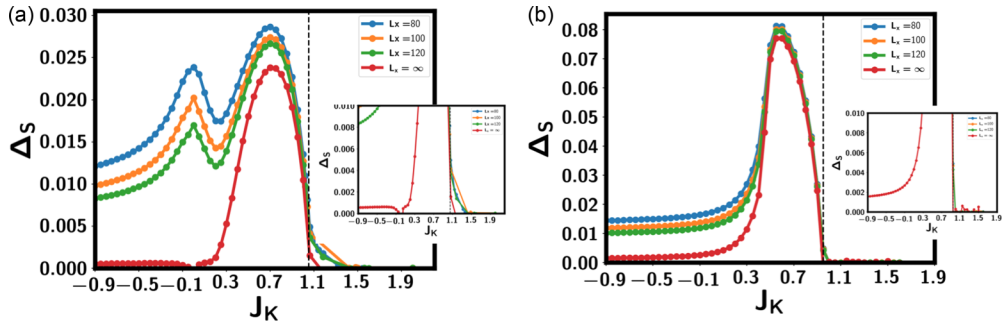

FIG. 9. Spin gap in the generalized Kondo model from finite DMRG at $x = 0.9$ for (a) $J_{cs} = 0$ and (b) $J_{cs} = 0.2$. We use parameter $t = 1, J_c = J_s = 0.5$. The value at $L = \infty$ is extracted from polynomial fitting $\Delta_S(\frac{1}{L_x}) = a\frac{1}{L_x^2} + b\frac{1}{L_x} + \Delta_S(L_x = \infty)$. In the inset we show a zoom in scale to demonstrate a finite spin gap at negative J_K regime.

$J_{cs} = 0, 0.25$, respectively. When $J_K > J_K^c$, we have a Luttinger liquid phase with zero spin gap. We note that the spin gap is finite even at negative J_K regime, though it is very small. The spin gap at $J_K = -\infty$ can get enhanced if we increase x or J_{cs}, as demonstrated in Fig. 10.

In addition to results from finite DMRG, we can also obtain correlation lengths using the transfer matrix techniques in infinite DMRG, as shown in Fig. 11. We mainly care about the spin correlation length ξ_S, obtained in the sector with $(\delta Q, \delta S_z) = (0, 1)$and the pairing correlation length ξ_P, obtained in the sector with $(\delta Q, \delta S_z) = (2, 0)$. We show the data for $J_{cs} = 0, 0.25, 0.5$. One can see that there is a finite ξ_S^{-1} when $J_K < J_K^c$, consistent with a spin gap. The pairing correlation length ξ_P increases with the bond dimension m. At a fixed m, ξ_P has a dip at J_K^0, where the Luttinger parameter K_c also has a dip and the pairing correlation function power-law decay exponent $K_{sc} = K_c^{-1}$ is peaked. This is another evidence that there are two superconducting domes separated by J_K^0.

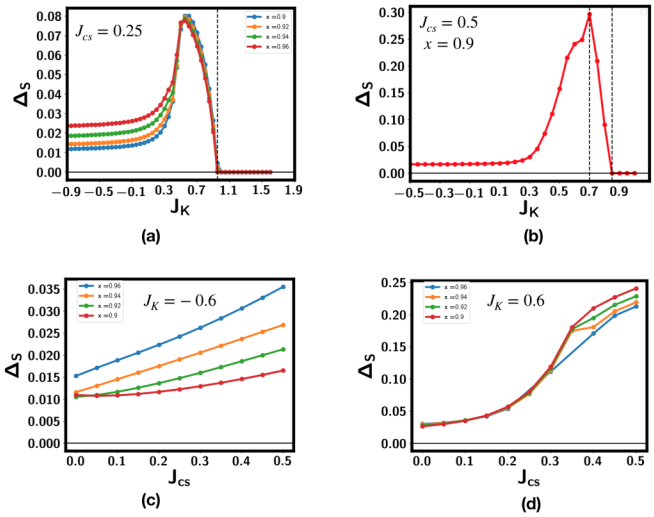

FIG. 10. (a) Spin gap with J_K at $J_{sc} = 0.25$, obtained with system size $L_x = 100$. (b) Spin gap with J_K at $J_{cs} = 0.5$ and $x = 0.9$. It is extrapolated to $L_x = \infty$ from data at $L_x = 80, 100, 120$. (c) Spin gap with J_{cs} at $J_K = -0.6$. (d) Spin gap with J_{cs} at $J_K = 0.6$.

3. Luttinger parameter K_c

In Fig. 12 we show the Luttinger parameter K_c with J_K. The Luttinger parameter K_c is fit using the method described in Appendix B. K_c clearly has a dip at $J_K = J_K^0$, The PDW phase is separated into two domes. For the special case with $J_{cs} = 0$, the $J_K^0 = 0$ point has zero spin gap and is a LL* phase with one charge mode and two spin modes. However, with a finite J_{cs}, the phase at J_K^0 is generically also in the same Luther-Emery liquid phase with spin gap, although K_c is smaller than one.

4. Charge compressibility and Fermi velocity

We also report the inverse charge compressibility κ_c^{-1} and the Luttinger parameter K_c in Fig. 13. By using $\kappa_c = \frac{2K_c}{\pi v_c}$, we can also obtain the Fermi velocity v_c and the charge stiffness $D = K_c v_c$. We can see that there is a dip of K_c and peak of the Fermi velocity v_c at J_K^0, where the spin-spin correlation $\langle \vec{S}_{i;c} \cdot \vec{S}_{i;s} \rangle$ changes sign. Away from the J_K^0, K_c gets enhanced and the Fermi velocity gets reduced, which is a signature of attractive interaction [21]. If we stay in the FM or AF regimes with fixed sign of $\langle \vec{S}_{i;c} \cdot \vec{S}_i \rangle$, then J_{cs} term enhances K_c and suppresses v_c, indicating stronger attraction. However, in Fig. 13(d), we find a dip of K_c at $J_{cs} \approx 0.4$. This is again associated with the sign change of $\langle \vec{S}_{i;c} \cdot \vec{S}_{i;s} \rangle$ and vanishing of the polaron hybridization because we expect $J_K^0 \approx 0.6$ when $J_{cs} = 0.4$ based on the data in Fig. 11.

APPENDIX D: SPIN POLARON AND ITS CORRELATION FUNCTIONS

In this section we show evidences for fermionic spin polaron at low energy and composite Cooper pair formed as bipolarons in the generalized Kondo model.

In the generalized Kondo model [Eq. (1)], the fermionic spin polaron is defined as

$$\tilde{c}_{i;\sigma} = \frac{1}{2}(\vec{S}_{i;s} \cdot \vec{\sigma}_{\sigma\sigma'})c_{i;\sigma'}, \tag{D1}$$

where $\vec{S}$ is the spin operator in the S layer and $c_{i;\sigma}$ is electron in the C layer. $\vec{\sigma}$ is the Pauli matrix which acts on the spin index of the electron operator. It is easy to show that the spin polaron operator $\tilde{c}_\sigma$ has the same quantum number as the microscopic electron operator c_σ.

With the interlayer spin-spin correlation, the polaron $\tilde{c}_{i;\sigma}$ will have finite overlap with the microscopic electron $c_{i;\sigma}$.

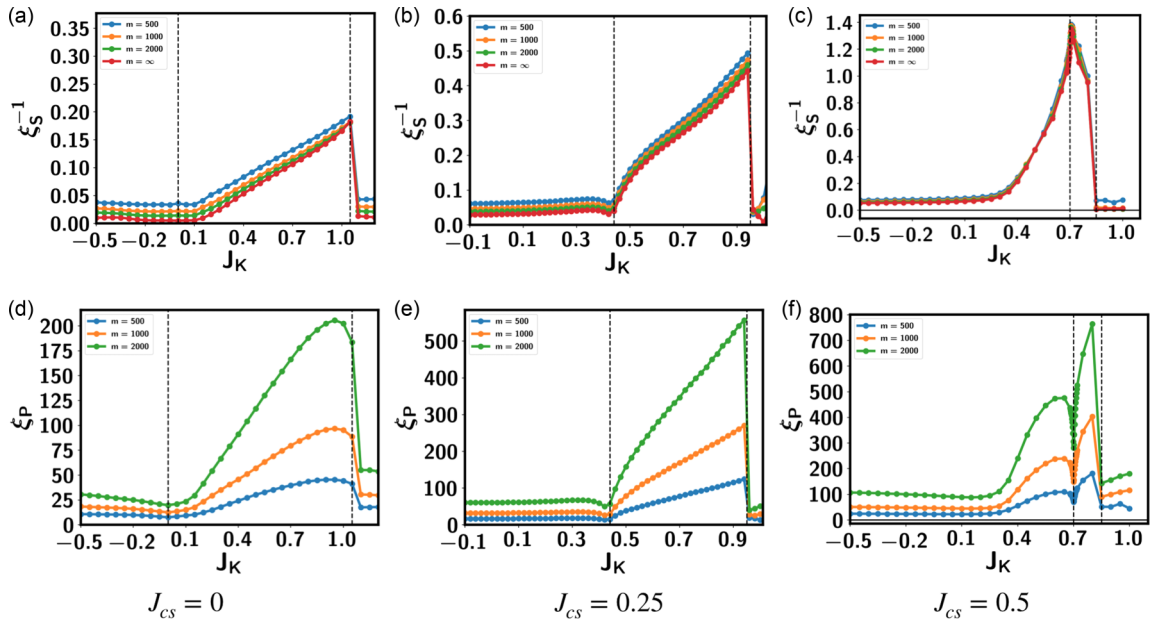

FIG. 11. Correlation lengths in infinite DMRG calculation at $x = \frac{28}{30}$ with unit cell size $L = 30$. We use $t = 1, J_c = J_s = 0.5$. Correlation length is obtained from the transfer matrix method in one specific sector. The spin correlation length ξ_S is from the sector $(\delta Q, \delta S_z) = (0, 1)$. The typical operator in this sector is the S^+ operator. The pairing correlation length ξ_P is from the sector $(\delta Q, \delta S_z) = (2, 0)$, with the typical operator as the Cooper pair operator. m is the bond dimension. $\xi_S^{-1}(m = \infty)$ is extrapolated from the relation $\xi_S^{-1}(\frac{1}{m}) = a\frac{1}{m^2} + b\frac{1}{m} + \xi_S^{-1}(m = \infty)$. (a, d) $J_{cs} = 0$. (b, e) $J_{cs} = 0.25$. (c, f) $J_{cs} = 0.5$. The two dashed lines are at J_K^0 and J_K^c.

Actually, one can find the hybridization to be

$$\sum_{\sigma=\uparrow,\downarrow} c^\dagger_{i;\sigma}\tilde{c}_{i;\sigma} = \vec{S}_{i;s}\cdot\vec{S}_{i;c}, \tag{D2}$$

which is nothing but the onsite interlayer spin-spin correlation. Here $\vec{S}_{i;c} = \frac{1}{2}c^\dagger_{i;\sigma}\vec{\sigma}_{\sigma\sigma'}c_{i;\sigma'}$ is the spin operator for the itinerant electron in the C layer.

1. Green functions of electron and polaron

We define electron-electron Green functions

$$G_{\sigma;ee}(x, y) = \langle c^\dagger_\sigma(x)c_\sigma(y)\rangle. \tag{D3}$$

Electron-polaron function:

$$G_{\uparrow;ep}(x, y) = \langle c^\dagger_\uparrow(x)c_\uparrow(y)S_z(y)\rangle_c + \langle c^\dagger_\uparrow(x)c_\downarrow(y)S^-(y)\rangle_c \tag{D4}$$

and

$$G_{\downarrow;ep}(x, y) = -\langle c^\dagger_\downarrow(x)c_\downarrow(y)S_z(y)\rangle_c + \langle c^\dagger_\downarrow(x)c_\uparrow(y)S^+(y)\rangle. \tag{D5}$$

Finally, polaron-polaron function:

$$G_{\uparrow;pp} = \langle c^\dagger_\uparrow(x)c_\uparrow(y)S_z(x)S_z(y)\rangle_c + \langle c^\dagger_\downarrow(x)c_\downarrow(y)S^\dagger(x)S^-(y)\rangle_c + \langle c^\dagger_\uparrow(x)c_\downarrow(y)S_z(x)S^-(y)\rangle_c + \langle c^\dagger_\downarrow(x)c_\uparrow(y)S^\dagger(x)S_z(y)\rangle_c,$$

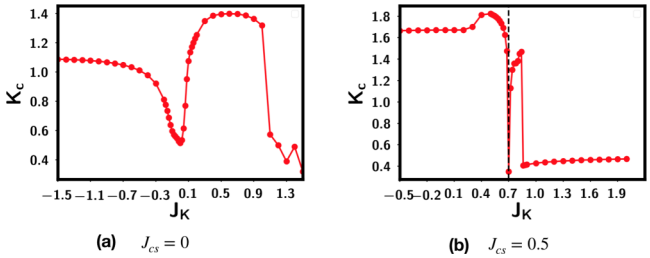

FIG. 12. Extracted Luttinger parameter K_c from finite DMRG at $L_x = 100$ and $x = 0.96$. (a) $J_{cs} = 0$, (b) $J_{cs} = 0.5$. The dashed line is at $J_K^0 = 0.7$ for $J_{cs} = 0.5$.

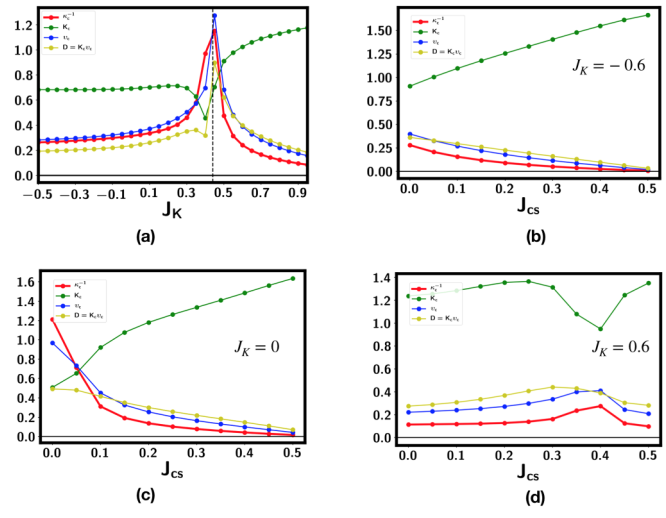

FIG. 13. Charge compressibility κ_c, luttinger parameter K_c, charge Fermi velocity υ_c, and charge stiffness $D = K_c\upsilon_c$. (a) Finite DMRG at $x = 0.94$ with system size $L_x = 100$ and $J_{cs} = 0.25$. (b, c, d) Change with J_{cs} at fixed $J_K = -0.6, 0, 0.6$ for density $x = 0.94$ with $L_x = 100$.

$$G_{\downarrow;pp} = \langle c^\dagger_\downarrow(x)c_\downarrow(y)S_z(x)S_z(y)\rangle + \langle c^\dagger_\uparrow(x)c_\uparrow(y)S^-(x)S^+(y)\rangle - \langle c^\dagger_\downarrow(x)c_\uparrow(y)S_z(x)S^+(y)\rangle - \langle c^\dagger_{i;\uparrow}c_{j;\downarrow}S^-(x)S_{j;z}\rangle_c. \tag{D6}$$

In the above $\vec{S}_i$ is the operator of the S layer only and $c_{i;\sigma}$ is the operator in the C layer. $\langle O_C O_S\rangle_c = \langle O_C O_S\rangle - \langle O_C\rangle\langle O_S\rangle$, where O_C and O_S are the operators in the C and S layer, respectively.

Inside the PDW phase, we find that

$$G_\alpha(x) = A_\alpha e^{-\frac{x}{\xi_\alpha}}, \tag{D7}$$

where $\alpha = ee, ep, pp$.

We always find that ξ_α is the same for all these three Green functions, therefore we believe that the polaron and the electron both have overlaps with the same low energy mode. The amplitude A_α/A_{ee} for $\alpha = ep, pp$ thus are characterizations of the mixture between the polaron and the electron.

2. Pairing-pairing correlation function for composite Cooper pair

With the spin polaron, it is easy to find that the spin-singlet pairing between electron and polaron:

$$\epsilon_{\sigma\sigma'}(c_{i;\sigma}\tilde{c}_{j;\sigma'} + \tilde{c}_{i;\sigma}c_{j;\sigma}) = \mathbf{\Delta}_{T;ij}\cdot(\mathbf{S}_{i;s} - \mathbf{S}_{j;s}), \tag{D8}$$

where the spin-triplet order parameters are

$$\mathbf{\Delta}_T = (c_{i;\downarrow}c_{j;\downarrow} - c_{i;\uparrow}c_{j;\uparrow}, -i(c_{i;\uparrow}c_{j;\uparrow} + c_{i;\downarrow}c_{j;\downarrow}), c_{i;\uparrow}c_{j;\downarrow} + c_{i;\downarrow}c_{j;\uparrow}). \tag{D9}$$

We can also define spin-singlet pairing between polarons:

$$\epsilon_{\sigma\sigma'}\tilde{c}_{i;\sigma}\tilde{c}_{j;\sigma'} = -\Delta_{S;ij}(\mathbf{S}_{i;s}\cdot\mathbf{S}_{j;s}) + i\mathbf{\Delta_{T;ij}}\cdot(\mathbf{S}_{i;s}\times\mathbf{S}_{j;s}). \tag{D10}$$

If we define the Neel order parameter $\vec{n}(x) = (-1)^x[\vec{S}(x) - \vec{S}(x+1)]$ and the VBS order parameter $\tilde{V}(x) = (-1)^x\vec{S}(x)\cdot\vec{S}(x+1)$ in the S layer, then we can see that the composite Cooper pairing order parameter $\vec{\Delta}_T\cdot\vec{n}$ can be understood as the Cooper pairing of one electron and one spin polaron and the composite pairing order $\Delta_S\tilde{V}$ is formed as a Cooper pair of spin polarons.

Motivated by this observation, in addition to the usual spin-singlet Cooper pair $\Delta(x) = \epsilon_{\sigma\sigma'}c_\sigma(x)c_{\sigma'}(x+1)$, we can define another two composite pairing order parameter: $\Delta_1(x) = \frac{1}{3}\vec{\Delta}_T(x)\cdot[\vec{S}(x) - \vec{S}(x+1)]$ and $\Delta_2(x) = \Delta(x)\vec{S}(x)\cdot\vec{S}(x+1)$. Here $\vec{S}(x)$ is the spin operator for the S layer only. If we use spin rotation symmetry, then we can further use $\Delta_1(x) = \Delta_{T;z}(x)[S_z(x) - S_z(x+1)]$.

Given that spin polaron is mixed with the single electron, we expect that Δ_1, Δ_2 are also mixed with the usual Cooper pair Δ. To characterize the mixture, we define the corresponding pairing-pairing correlation functions:

$$\langle\Delta^\dagger_\alpha(x)\Delta_\alpha(0)\rangle_c = A_\alpha\frac{(-1)^x}{x^{K_{sc;\alpha}}}. \tag{D11}$$

Again $\langle O(x)O(0)\rangle_c$ is defined by subtracting the connected part so that it is zero at the decoupled limit $J_{cs} = J_K = 0$ for $\alpha = \Delta_1, \Delta_2$. Within the PDW phase, we find that K_{sc} is the same for all these three correlation functions labeled

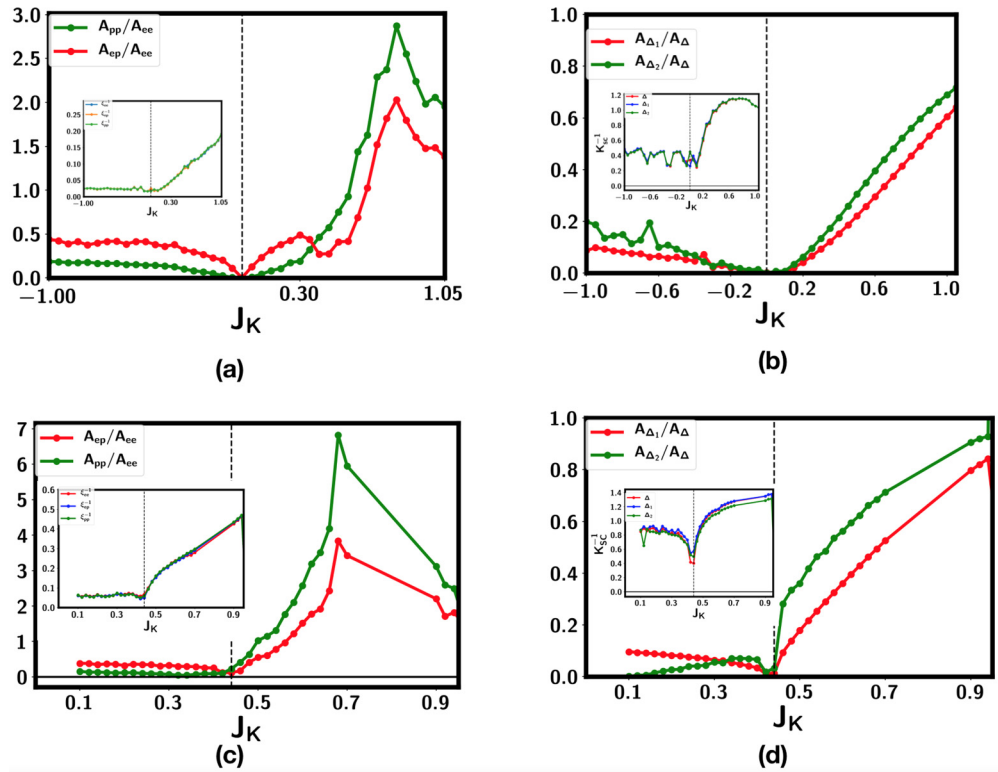

FIG. 14. Amplitudes and exponents for Green functions and pair-pair correlation functions obtained from infinite-DMRG with unit cell size $L = 30$ and $x = \frac{28}{30} \approx 0.933$. (a, b) $J_{cs} = 0$. The dashed line is at $J_K^0 = 0$. (c, d) $J_{cs} = 0.25$. The dashed line is at $J_K^0 = 0.44$. Panels (a, c) are for Green functions defined in Appendix D 1. (b, d) are for pairing correlation functions defined in Appendix D 2.

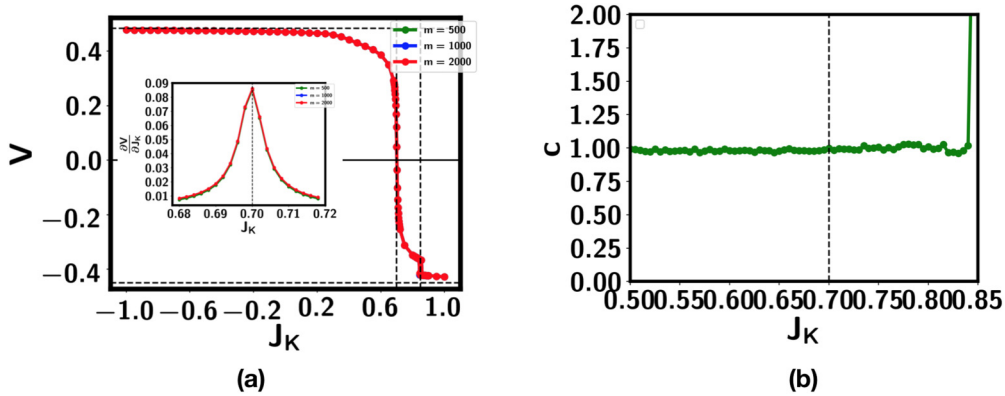

FIG. 15. (a) $\langle V_i \rangle$ for $J_{cs} = 0.5$ from infinite DMRG. We use $x = \frac{14}{15}$ with unit cell size $L = 30$. (b) Central charge c fit from entanglement entropy $S = \frac{c}{6} \log \xi$, where ξ is the correlation length. The two dashed lines are at $J_K^0 = 0.7$ and $J_K^c = 0.85$.

by $\alpha = \Delta, \Delta_1, \Delta_2$, consistent with the expectation that they correspond to the same low energy mode. The amplitudes $\frac{A_{\Delta_1}}{A_\Delta}$ and $\frac{A_{\Delta_2}}{A_\Delta}$ are then characterizations of the presence of the electron-polaron pair Δ_1 and polaron-polaron pair Δ_2.

3. Numerical results

In Fig. 14 we show the amplitudes of the Green function and the pairing correlation functions defined in the previous two subsections. We can see that the amplitude of the polaron Green function and the polaron-polaron pairing correlation has a dip at J_K^0, where the Luttinger parameter K_c also has a dip. This is an indication that the existences of the fermionic spin polaron and bipolarons are important to make $K_c < 1$, which is required to get slow decay of the pairing correlation.

APPENDIX E: RAPID CROSSOVER AT J_K^0

As shown in the previous sections, there is a dip of the Luttinger parameter K_c at J_K^0, which separates the PDW phase into two regimes. These two regimes have $\langle \vec{S}_{i;c} \cdot \vec{S}_i \rangle > 0$ and $\langle \vec{S}_{i;c} \cdot \vec{S}_i \rangle < 0$ separately. Here we address the question on whether there is a phase transition between the ferromagnetic and antiferromagnetic regimes of the PDW phase. Our conclusion is that there is only a rapid crossover and there is no phase transition happening at J_K^0. We have already shown the change of $\langle V_i \rangle = \langle \vec{S}_{i;c} \cdot \vec{S}_{i;s} \rangle + \frac{1}{4}$ for $J_{cs} = 0.25$ in the main text. In Fig. 15 we show that for $J_{cs} = 0.5$. We can see that V has a rapid change at $J_K^0 = 0.7$. V is the first derivative of the energy with J_K, so the continuity of V around J_K^0 rules out first order transition. $\frac{\partial V}{\partial J_K}$ has a peak but does not diverge with the bond dimension m, ruling out a second order phase transition. In Fig. 15(b), we can see that the central charge is $c = 1$ across J_K^0, strongly suggesting that there is no true phase transition.

However, we find that there is a change in the entanglement spectrum at J_K^0, as shown in Fig. 16. Here for each J_K, we label the entanglement spectrum λ_i with two colors for the two fermion parity. When $J_K < J_K^c$, we can see that one fermion parity has even fold degeneracy, while the other one has odd fold degeneracy. Across J_K^0, the degeneracy of the lowest level changes from twofold to onefold. Despite this entanglement transition, we believe the system does not have a true phase transition. Also, we do not find any boundary states at zero energy with open boundary for $J_K < J_K^c$, consistent with the earlier discovery that the PDW is not topological [24]. Entanglement transition without boundary mode and true phase transition has also been reported in a different model [37].

APPENDIX F: MORE RESULTS ON THE TYPE II *t-J* MODEL

In this section we provide more data on the type II t-J model in one dimension. In Fig. 17 we show the doping dependence for the spin gap, the Luttinger parameter K_c and the charge compressibility for the parameter $t = 1, J_s = J_d = 0.5, J_{sd} = 0.25$. We can see that there is an onset of the spin gap at $x_c = 0.85$. When $x > 0.85$, there is a quick increase of the Luttinger parameter K_c. We also find that the charge compressibility diverges when $x > 0.93$. This may suggest a phase separation phase, although the density profile in our finite DMRG calculation does not show phase separation and various correlation functions still look like a PDW phase. The charge compressibility is $\kappa_c = \frac{2K_c}{\pi v_c}$ and a divergent κ_c is associated with either a divergent of K_c or vanishing of the velocity v_c. We fit v_c from κ_c and K_c and find it indeed vanishes after $x > 0.93$. A rapid increase of K_c and divergence of κ_c has been also found in the conventional t-J model in 1D when increasing J/t to very large value [40]. But there it needs $J/t > 1$ which is unrealistic. In our model, we find a rapid increase of K_c even with realistic value of $J/t = 0.5$. It may suggest that there is a much larger attractive interaction in the type II t-J model compared to the conventional t-J model.

One may question the existence of a stable PDW phase because the divergence of the charge compressibility would lead to a phase separated phase. Here we point out that a Luther-Emery liquid phase with a finite spin gap and finite charge compressibility exist in the range $0.85 < x < 0.93$ in Fig. 17. For this particular example it seems that $K_c < 1$ in the region with finite κ_c. However, this may be just a coincidence. For example, if we use $t = 1, J_s = J_d = 0.3, J_{sd} = 0.15$, then we find that κ_c is finite and $v_c > 0$ for $x < 0.975$ beyond which we do not have data. So there is no instability to phase separation for $x < 0.975$, but we can still find $K_c > 1$, as shown in Fig. 18. It is not clear whether a divergence of κ_c will happen at larger x. In other words, whether we always have a phase separated regime between the PDW phase and the Haldane chain insulator at $x = 1$ remains as an open question.

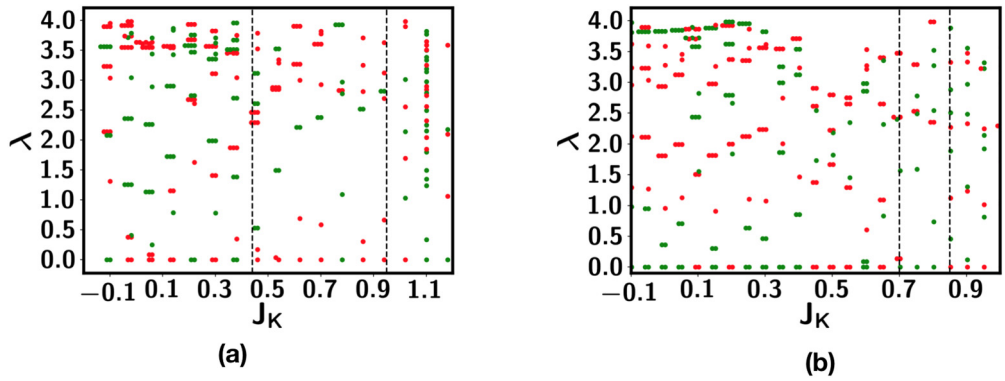

FIG. 16. Entanglement spectrum with J_K. (a) $J_{cs} = 0.25$. The two dashed lines are at $J_K^0 = 0.44$ and $J_K^c = 0.95$. (b) $J_{cs} = 0.5$. The two dashed lines are at $J_K^0 = 0.7$ and $J_K^c = 0.95$.

A rapid increase of K_c suggest a decrease of the exponent K_{sc} corresponding to the algebraic decay of the pairing-pairing correlation function. We indeed find this behavior by explicitly fitting K_{sc}, shown in Fig. 19 for $J_s = J_d = 2J_{sd} = 0.5$. In the regime $x < x_c$ (with $x_c \approx 0.85$), K_{sc} is slightly larger than 2, consistent with the result $K_{sc} = 1 + \frac{1}{K_c}$ with $K_c < 1$ for a Luttinger liquid phase with repulsive interaction. However, when $x > x_c$, K_{sc} quickly drops and approaches zero in the $x \to 1$ limit. This is consistent with the expectation $K_{sc} = \frac{1}{K_c}$ and the behavior of K_c shown in Fig. 17.

The PDW superconductor has a momentum $\mathbf{q} = \pi$, as shown in the peak at $\mathbf{q} = \pi$ of $P^\dagger(q)P(-q)$ in Fig. 20(d). Here $P^\dagger(q)P(-q)$ is the Fourier transformation of $P^\dagger(r)P(0)$, which is the correlation function of spin-singlet Cooper pair between nearest-neighbor sites. Inside the PDW phase, the density-density correlation function $\langle \delta N(q)\delta N(-q)\rangle$ shows peak at $q = \frac{1+x}{2} \times 2\pi$. In contrast, the peak is at either $2k_F$ or $4k_F$ with $2k_F = \frac{x}{2} \times 2\pi$ inside the LL* phase. This behavior can be captured in the bosonization theory provided in Appendix G.

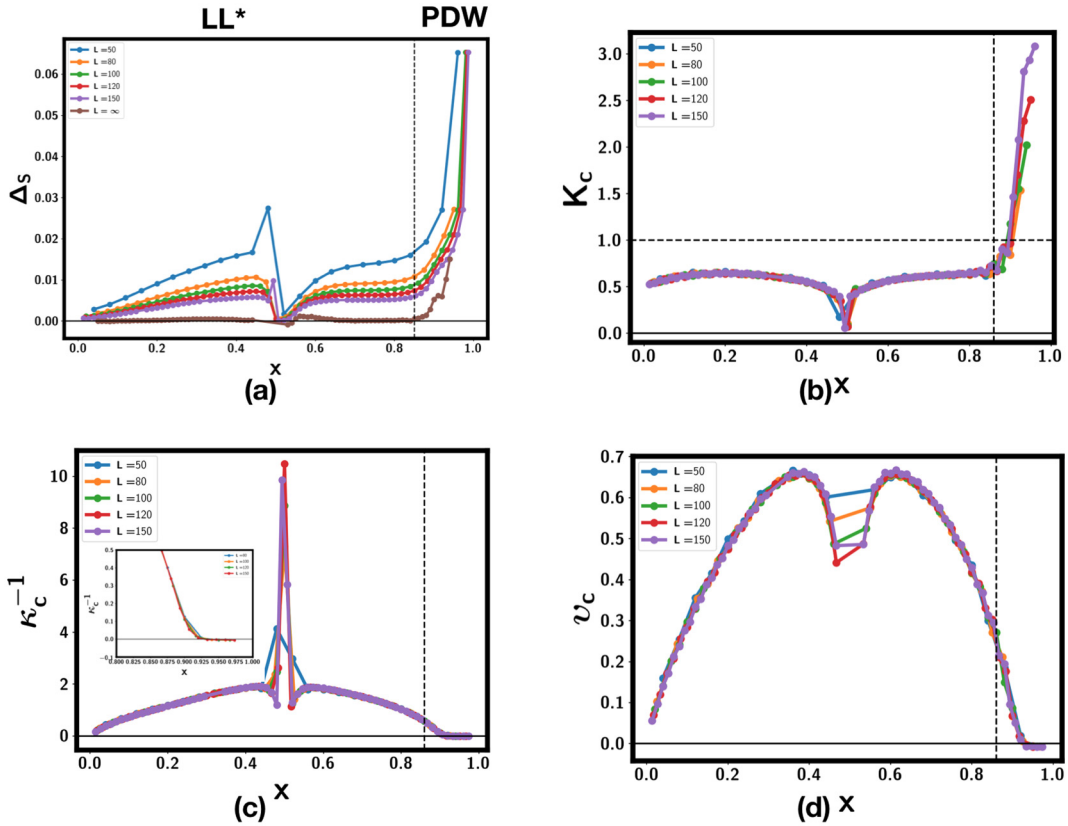

FIG. 17. Doping dependence in the type II t-J model with $t = 1, J_s = J_d = 0.5, J_{sd} = 0.25$ from finite DMRG calculation. (a) Spin gap Δ_S; (b) the Luttinger parameter K_c for the charge mode; (c) the charge compressibility κ_c; (d) the Fermi velocity of the charge mode v_c fit from $\kappa_c = \frac{2K_c}{\pi v_c}$. $x = 0.5$ is in a CDW phase and therefore there is discontinuity at this filling.

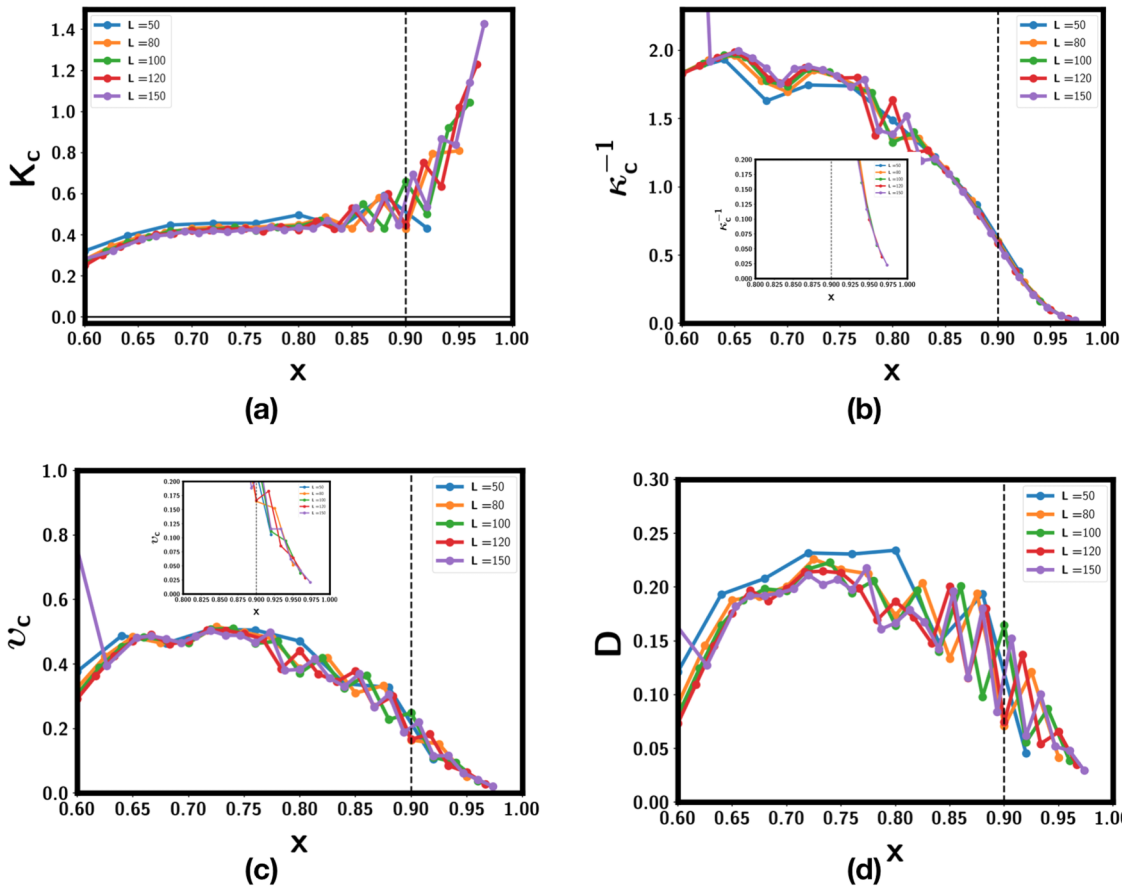

FIG. 18. Doping dependence in the type II t-J model with $t = 1, J_s = J_d = 0.3, J_{sd} = 0.15$ from finite DMRG calculation. In this case we do not find the divergence of the charge compressibility in the density range we can reach.

APPENDIX G: BOSONIZATION THEORY OF PDW AND ITS TRANSITION TO LL* PHASE

We provide a bosonization theory of the 1D PDW superconductor and its transition to the LL* phase. A very similar analysis has been performed for a two-leg Hubbard model in Ref. [34]. For simplicity, we consider the generalized Kondo model in Eq. (A1). In the limit $J_H = J_{cs} = 0$, the phase is apparently in a LL* phase with a conventional spinful Luttinger liquid decoupled plus a spin-1/2 chain.

For the itinerant electron in the C layer, we have bosonization mapping:

$$\psi_{r\sigma} = \frac{1}{\sqrt{2\pi\alpha}} U_{r,\sigma} e^{irk_F x} e^{-\frac{i}{\sqrt{2}}[r\phi_c - \theta_c + \sigma(r\phi_s - \theta_s)]}, \tag{G1}$$

where $r = R, L$ labels the right-moving and the left-moving modes. $\sigma = \uparrow, \downarrow$ labels the spin. $U_{r,\sigma}$ is the Klein factor.

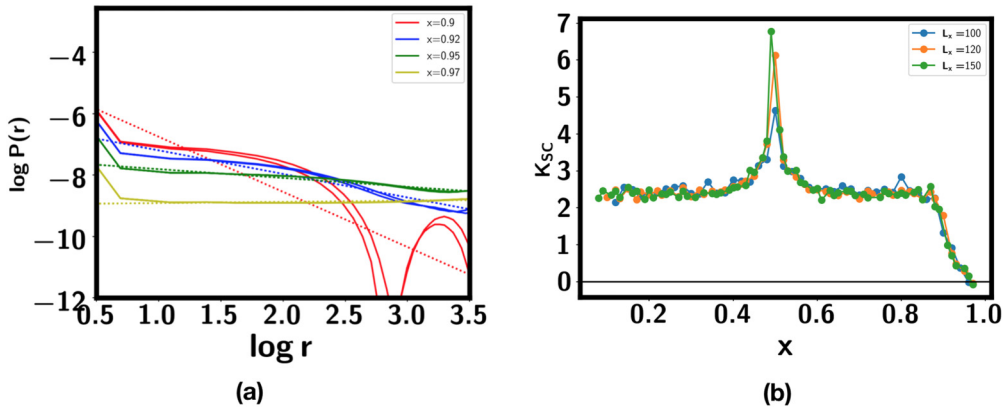

FIG. 19. (a) $\log|P(r)|$ vs $\log r$, where $P(r) = \langle\Delta_S(r)\Delta_S(0)\rangle$ is the pairing-pairing correlation function. The dashed lines correspond to linear fit line whose exponent gives K_{sc}. (b) Doping dependence of the superconductor decaying exponent K_{sc} for the type II t-J model.

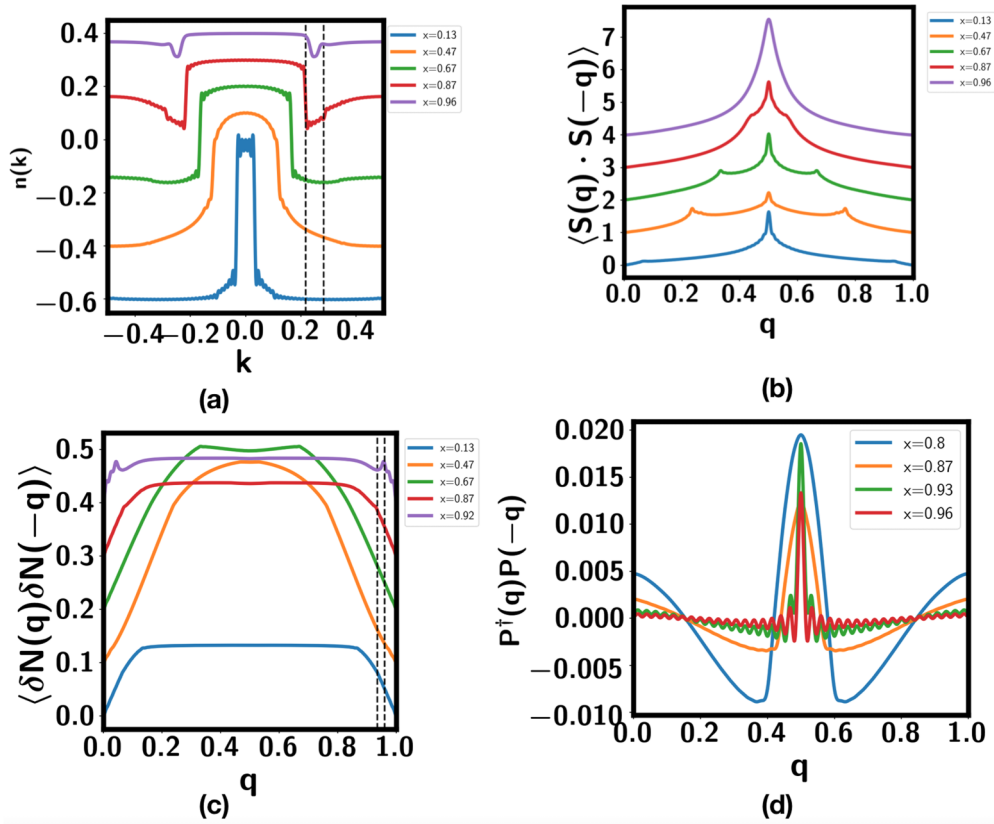

FIG. 20. Doping dependence of various correlation functions. (a) Momentum distribution function $n(k) = \sum_\sigma c_\sigma^\dagger(k)c_\sigma(k)\rangle$. There is a small Fermi surface with $k_F = \frac{x}{4} \times 2\pi$ which expands with x. When x is large, there is also feature at $k_F + \pi$ from the scattering of the spin mode with $q = \pi$. The two dashed lines are at $k = k_F$ and $k = k_F + \pi$ at $x = 0.85$. (b) Structure factor of the spin-spin correlation function. In the LL* phase when $x < 0.85$, there are two modes at $q = 2k_F = \frac{x}{2} \times 2\pi$ and at $q = \pi$. (c) Density-density structure factor. The two dashed lines correspond to $q = \frac{1+x}{2} \times 2\pi$ for $x = 0.87$ and $x = 0.92$. (d) $\langle P^\dagger(\mathbf{q})P(-q)\rangle$, where $P(q)$ is Fourier transformation of the spin-singlet Cooper pair. Momentum is in units of 2π.

Similarly, for the localized spin-1/2 chain in the S layer, we have a spin mode $\tilde{\theta}_s, \tilde{\phi}_s$, while the corresponding charge mode $\tilde{\theta}_c, \tilde{\phi}_c$ is gapped ($\tilde{\phi}_c = 0$) because it is in a Mott insulator.

At $J_{cs} = 0$, the Hamiltonian is

$$H = \frac{\upsilon_c}{2\pi}\int dx K_c(\partial_x\theta_c)^2 + \frac{1}{K_c}(\partial_x\phi_c)^2 + \frac{\upsilon_s}{2\pi}\int dx(\partial_x\theta_s)^2 + (\partial_x\phi_s)^2 + \frac{\tilde{\upsilon}_s}{2\pi}\int dx(\partial_x\tilde{\theta}_s)^2 + (\partial_x\tilde{\phi}_s)^2, \tag{G2}$$

where we have assumed that the Luttinger parameter for the spin modes are $K_s = \tilde{K}_s = 1$ from the $SU(2)$ spin rotation symmetry. K_c is a function of J/t and x. In the following we just treat it as a phenomenological parameter. Note that for spin-1/2 chain in the S layer, we still use the convention that $K_s = 1$ instead of $K = 1/2$ as derived from fermionization of spin chain.

Next, we need to add the J_{cs} and $J_K = -J_H$ terms. To do that, we need to represent the electron spin $\mathbf{S}_{i;c}$ and the local spin $\mathbf{S}_i$ with the bosonization language. First, the spin of the C layer is

$$\begin{aligned} S_c^z &= -\frac{1}{\sqrt{2\pi}}\partial_x\phi_s + \frac{1}{2\pi\alpha}\left(e^{-2ik_Fx}e^{i\sqrt{2}\phi_c}\frac{1}{2}(\eta_1\eta_3 e^{i\sqrt{2}\phi_s} - \eta_2\eta_4 e^{-i\sqrt{2}\phi_s}) + \text{H.c.}\right), \\ S_c^+ &= \frac{1}{2\pi\alpha}(\eta_1\eta_4 e^{-i2k_Fx}e^{-i\sqrt{2}\theta_s}e^{i\sqrt{2}\phi_c} + \eta_3\eta_2 e^{i2k_Fx}e^{-i\sqrt{2}\theta_s}e^{-i\sqrt{2}\phi_c} + \eta_1\eta_2 e^{-i\sqrt{2}\theta_s}e^{i\sqrt{2}\phi_s} + \eta_3\eta_4 e^{-i\sqrt{2}\theta_s}e^{-i\sqrt{2}\phi_s}), \end{aligned} \tag{G3}$$

where $2k_F = \frac{x}{2}2\pi$. $\eta_1, \eta_2, \eta_3, \eta_4$ are the Klein factors introduced to fix the fermion statistics. We fix the gauge $\eta_1\eta_2\eta_3\eta_4 = 1$. For spin operators, the Klein factors can be suppressed by setting $\eta_1\eta_3 = \eta_2\eta_4 = -i$, $\eta_1\eta_2 = -\eta_3\eta_4 = -i$ and $\eta_1\eta_4 = \eta_3\eta_2 = i$ [41]. Then we get

$$\begin{aligned} S_c^z &= -\frac{1}{\sqrt{2\pi}}\partial_x\phi_s + \frac{1}{2\pi\alpha}\sin\sqrt{2}\phi_s(e^{-2ik_Fx}e^{i\sqrt{2}\phi_c} + e^{2ik_Fx}e^{-i\sqrt{2}\phi_c}), \\ S_c^+ &= \frac{1}{2\pi\alpha}i(e^{-i2k_Fx}e^{-i\sqrt{2}\theta_s}e^{i\sqrt{2}\phi_c} + e^{i2k_Fx}e^{-i\sqrt{2}\theta_s}e^{-i\sqrt{2}\phi_c}) + e^{-i\sqrt{2}\theta_s}\sin\sqrt{2}\phi_s. \end{aligned} \tag{G4}$$

For the local spin $\vec{S}_i$, we can use the same expression with spin mode $\tilde{\theta}_s$, $\tilde{\phi}_s$. This gives

$$\tilde{S}_z = -\frac{1}{\sqrt{2}\pi}\partial_x\tilde{\phi}_s + (-1)^x\frac{1}{2\pi\alpha}\sin\sqrt{2}\tilde{\phi}_s, \quad \tilde{S}^+ = \frac{1}{2\pi\alpha}((-1)^x ie^{-i\sqrt{2}\tilde{\theta}_s} + e^{-i\sqrt{2}\tilde{\theta}_s}\sin\sqrt{2}\tilde{\phi}_s). \tag{G5}$$

Finally, we can write the interlayer spin-spin coupling as

$$H' = \frac{g}{2\pi^2}\int dx\partial_x\phi_s\partial_x\tilde{\phi}_s - \frac{g}{8\pi^2\alpha^2}\int dx\cos 2\theta_{s;-}\cos 2\phi_{s;+} + \frac{g}{8\pi^2\alpha^2}\int dx\cos 2\theta_{s;-}\cos 2\phi_{s;-}, \tag{G6}$$

where $g = 2J_{cs} - J_H$ and $g' = 2J_{cs} - J_H$. We defined $\theta_{s;\pm} = \frac{1}{\sqrt{2}}(\theta_s \pm \tilde{\theta}_s)$ and $\phi_{s;\pm} = \frac{1}{\sqrt{2}}(\phi_s \pm \tilde{\phi}_s)$.

The first line will renormalize the Luttinger parameter $K_\pm$ for the $\theta_{s;\pm}$ mode. For simplicity we assume $\upsilon_s = \tilde{\upsilon}_s = \upsilon$ at the initial point. We will have

$$H = \frac{\upsilon_c}{2\pi}\int dxK_c(\partial_x\theta_c)^2 + \frac{1}{K_c}(\partial_x\phi_c)^2 + \frac{\upsilon_+}{2\pi}\int dxK_+(\partial_x\theta_{s;+})^2 + \frac{1}{K_+}(\partial_x\phi_{s;+})^2 + \frac{\upsilon_-}{2\pi}\int dxK_-(\partial_x\theta_{s;-})^2 + \frac{1}{K_-}(\partial_x\phi_{s;-})^2$$
$$- \frac{g}{8\pi^2\alpha^2}\int dx\cos 2\theta_{s;-}\cos 2\phi_{s;+} + \frac{g'}{8\pi^2\alpha^2}\int dx\cos 2\theta_{s;-}\cos 2\phi_{s;-}, \tag{G7}$$

where

$$\upsilon_\pm = \upsilon\sqrt{1 \pm \frac{g}{2\pi\upsilon}}, \quad K_\pm = \frac{1}{\sqrt{1 \pm \frac{g}{2\pi\upsilon}}}. \tag{G8}$$

Note that in the above we have ignored the intralayer spin-spin coupling. We assume that at the decoupled limit the intralayer super-exchange terms J_c, J_s are not strong enough to destroy the LL* phase. Here we are mainly interested in the possible instability of the LL* phase caused by the interlayer spin-spin coupling terms J_H and J_{cs}. The scaling dimension of g' is $[g'] = 2 - (K_- + \frac{1}{K_-}) < 0$ and the g' term is generically irrelevant. In the following we only keep the g term. The RG equation is

$$\frac{dK_+}{dl} = -\frac{1}{4}K_+^2g^2, \quad \frac{dK_-}{dl} = \frac{1}{4}g^2,$$
$$\frac{dg}{dl} = \left(2 - K_+ - \frac{1}{K_-}\right)g. \tag{G9}$$

We note that if $g > 0$ initially, then $K_+ + \frac{1}{K_-} < 2$ and g flows to $+\infty$. The g term will pin $\theta_{s;-}$ and $\phi_{s;+}$, so both spin modes are gapped out and we are left with only the charge mode θ_c, ϕ_c. This turns out to be a PDW superconducting phase which we will describe later. However, if $g < 0$, then $K_+ + \frac{1}{K_-} > 2$ initially and g flows to zero, while K_+, K_- flow to 1, resulting in the LL* phase. Therefore, changing g tunes a phase transition between the LL* phase and the PDW phase.

We note that the oscillating part of the spin operator in the C layer does not enter the final Hamiltonian because $2k_F = (1-x)\pi$ is incommensurate and can not cancel the $\mathbf{q} = \pi$ part of the $\tilde{S}$. In contrast, for the $x = 1$ point, the oscillatory part also enters the Hamiltonian and there is term like $-g_1\cos 2\phi_{s;+} - g_2\cos 2\phi_{s;-}$, which is more relevant than the g and g' term. Therefore, the above analysis only works for $x < 1$ and will break down for the filling $x = 1$, where we will get Mott insulator with spin in either Haldane phase or a rung-singlet phase.

The above analysis suggests that there is a Kosterlitz-Thouless (KT) transition between a LL* phase ($g < 0$) and a PDW phase ($g > 0$). The central charge changes from $c = 3$ to $c = 1$. The same transition has been found at $x_c = 0.85$ of the type II t-J model shown in Figs. 17 and 6. In the following we study the property of the PDW phase in details based on bosonization language.

1. Property and order parameter of the PDW phase

We discuss the property of the PDW superconductor phase in the $g > 0$ region. The $-g\cos 2\theta_{s;-}\cos 2\phi_{s;+}$ will pin $\theta_{s;-}$ and $\phi_{s;+}$ into either $\theta_{s;-} = \phi_{s;+} = 0$ or $\theta_{s;-} = \phi_{s;+} = \frac{\pi}{2}$. Next we will study various correlation functions and show that this is a PDW phase with a composite pairing operator.

Because only the charge mode survives, the phase must be a Luther-Emery liquid with a gap for spin and single electron excitation. The only order parameter we need to consider is the pairing order and the charge-density-wave (CDW) orders. Here we will show that the pairing and CDW order within the C layer is actually also gapped in the sense that its correlation function is exponentially decayed. The only gapless order parameter is a composite object by combining the order parameter in the C layer with the Neel or valence-bond-solid (VBS) order parameter in the S layer.

The zero-momentum spin-singlet superconductor order parameter within C layer is

$$\Delta_S = \psi_{R\uparrow}\psi_{L\downarrow} - \psi_{R\downarrow}\psi_{L\uparrow} = \frac{i}{\pi\alpha}e^{i\sqrt{2}\theta_c}\cos\sqrt{2}\phi_s, \tag{G10}$$

also zero-momentum spin-triplet pairing within C layer is

$$\mathbf{\Delta}_T = (\psi_{R\downarrow}\psi_{L\downarrow} - \psi_{R\uparrow}\psi_{L\uparrow}, -i(\psi_{R\uparrow}\psi_{L\uparrow} + \psi_{R\downarrow}\psi_{L\downarrow}),$$
$$\times\ \psi_{R\uparrow}\psi_{L\downarrow} + \psi_{R\downarrow}\psi_{L\uparrow})$$
$$= \frac{1}{\pi\alpha}e^{i\sqrt{2}\theta_c}(\sin\sqrt{2}\theta_s, \cos\sqrt{2}\theta_s, \sin\sqrt{2}\phi_s). \tag{G11}$$

We can write down density operator as

$$\rho(x) = -\frac{\sqrt{2}}{\pi}\partial_x\phi_c + e^{i2k_Fx}\rho_{2k_F}(x) + e^{-i2k_Fx}\rho_{-2k_F}, \tag{G12}$$

where the CDW order at momentum $Q = 2k_F = 2\pi\frac{x}{2}$ is

$$\rho_{2k_F}(x) = \frac{i}{\pi\alpha}e^{-i\sqrt{2}\phi_c}\cos(\sqrt{2}\phi_s). \tag{G13}$$

All of these order parameters contain terms like $\cos\sqrt{2}\phi_s$, $\cos\sqrt{2}\theta_s$, $\sin\sqrt{2}\phi_s$, and $\sin\sqrt{2}\theta_s$. Because $\phi_s = \frac{1}{\sqrt{2}}(\phi_{s;+} + \phi_{s;-})$ and $\theta_s = \frac{1}{\sqrt{2}}(\theta_{s;+} + \theta_{s;-})$, the correlation functions of these terms are exponentially decayed. This is because we can not pin $\phi_{s;+}, \phi_{s;-}$ at the same time. For example, let us consider $\cos\sqrt{2}\phi_s = \cos(\phi_{s;+} + \phi_{s;-})$. In the PDW phase, $\phi_{s;+}$ and $\theta_{s;-}$ is pinned, so $\phi_{s;-}$ is gapped. $\cos(\phi_{s;+} + \phi_{s;-}) \sim \cos\phi_{s;-}$ has exponentially decayed correlation function.

In the following we show that certain composite order parameter still has power-law correlation function. The key idea is to cancel the factor like $\cos(\phi_{s;+} + \phi_{s;-})$ by combining an order parameter from the S layer. First, in S layer we can define Neel order parameter through $\vec{S} = \vec{S}_0 + (-1)^x\vec{n}$. Here $\vec{n}$ is the Neel order parameter with a momentum $Q = \pi$. It is easy to find that $(n_x, n_y, n_z) = \frac{1}{2\pi\alpha}(\sin\sqrt{2}\tilde{\theta}_s, \cos\sqrt{2}\tilde{\theta}_s, \sin\sqrt{2}\tilde{\phi}_s)$. Meanwhile, there is a VBS order parameter defined through $\vec{S}_i \cdot \vec{S}_j \sim (-1)^i\tilde{V}$. The VBS order parameter V carries momentum $\mathbf{Q} = \pi$ and can be expressed as $\tilde{V} = \frac{1}{2\pi\alpha}\cos\sqrt{2}\tilde{\phi}_s$.

Now we can define a composite order parameter $\Delta_{\text{PDW}} \sim \Delta_S\tilde{V} \sim e^{i\sqrt{2}\theta_c}(\cos 2\phi_{s;+} + \cos 2\phi_{s;-})$. We note that $\phi_{s;+}$ is pinned while $\phi_{s;-}$ is fluctuating, so we only needs to keep $\cos 2\phi_{s;+}$ term which is basically a constant. In the end we find $\Delta_S\tilde{V} \sim e^{-i\sqrt{2}\theta_c}$. Actually, we can also find that $\vec{\Delta}_T \cdot \vec{n} \sim e^{-i\sqrt{2}\theta_c}$. Therefore, we have the composite PDW order parameter:

$$O_{\text{PDW}} \sim \Delta_S\tilde{V} \sim \vec{\Delta}_T \cdot \vec{n} \sim e^{-i\sqrt{2}\theta_c}, \tag{G14}$$

which carries momentum $Q_{\text{PDW}} = \pi$ and is spin singlet.

Similarly, one can define a composite CDW order parameter

$$O_{CDW} \sim \rho_{2k_F}(x)\tilde{V} \sim e^{-i\sqrt{2}\phi_c}, \tag{G15}$$

which carries momentum $Q_{\text{CDW}} = 2k_F + \pi = \frac{1+x}{2}2\pi$.

It is easy to find correlation function of the PDW and CDW order parameters:

$$O_{\text{PDW}}(x)O_{\text{PDW}}(0) \sim \frac{1}{x^{\frac{1}{K_c}}} \tag{G16}$$

and

$$O_{\text{CDW}}(x)O_{\text{CDW}}(0) \sim \frac{1}{x^{K_c}}. \tag{G17}$$

One can see that both the PDW and CDW order parameter have power-law decay correlation functions, though their exponents are inverse to each other. This is a typical behavior of Luther-Emery liquid. When x is close to 1, we find $K_c > 1$ in our DMRG calculation, thus PDW order dominates over the CDW order. This is the reason why we call the phase as PDW superconductor.

[1] P. A. Lee, N. Nagaosa, and X.-G. Wen, Rev. Mod. Phys. **78**, 17 (2006).
[2] F. D. M. Haldane, Phys. Rev. Lett. **50**, 1153 (1983).
[3] I. Affleck, J. Phys.: Condens. Matter **1**, 3047 (1989).
[4] I. Affleck, T. Kennedy, E. H. Lieb, and H. Tasaki, in *Condensed Matter Physics and Exactly Soluble Models* (Springer, Berlin, 2004), pp. 249–252
[5] Z.-C. Gu and X.-G. Wen, Phys. Rev. B **80**, 155131 (2009).
[6] F. Pollmann, A. M. Turner, E. Berg, and M. Oshikawa, Phys. Rev. B **81**, 064439 (2010).
[7] S.-Q. Ning, Z.-X. Liu, and H.-C. Jiang, Phys. Rev. Research **2**, 023184 (2020).
[8] A. Keselman, E. Berg, and P. Azaria, Phys. Rev. B **98**, 214501 (2018).
[9] Z. Zhu, D. N. Sheng, and Z.-Y. Weng, Phys. Rev. B **97**, 115144 (2018).
[10] H.-C. Jiang, Z.-X. Li, A. Seidel, and D.-H. Lee, Sci. Bull. **63**, 753 (2018).
[11] N. D. Patel, N. Kaushal, A. Nocera, G. Alvarez, and E. Dagotto, npj Quantum Mater. **5**, 27 (2020).
[12] N. D. Patel, A. Nocera, G. Alvarez, A. Moreo, and E. Dagotto, Phys. Rev. B **96**, 024520 (2017).
[13] P. Fazekas, *Lecture Notes on Electron Correlation and Magnetism*, Vol. 5 (World Scientific, Singapore, 1999).
[14] Y.-H. Zhang and A. Vishwanath, Phys. Rev. Research **2**, 023112 (2020).
[15] Y.-H. Zhang and Z. Zhu, Phys. Rev. B **103**, 115101 (2021).
[16] M. Gall, N. Wurz, J. Samland, C. F. Chan, and M. Köhl, Nature (London) **589**, 40 (2021).
[17] P. Sompet, S. Hirthe, D. Bourgund, T. Chalopin, J. Bibo, J. Koepsell, P. Bojović, R. Verresen, F. Pollmann, G. Salomon *et al.*, Nature (London) **606**, 484 (2022).
[18] D. F. Agterberg, J. S. Davis, S. D. Edkins, E. Fradkin, D. J. Van Harlingen, S. A. Kivelson, P. A. Lee, L. Radzihovsky, J. M. Tranquada, and Y. Wang, Annu. Rev. Condens. Matter Phys. **11**, 231 (2020).
[19] N. D. Patel, A. Nocera, G. Alvarez, R. Arita, A. Moreo, and E. Dagotto, Phys. Rev. B **94**, 075119 (2016).
[20] J. Herbrych, M. Środa, G. Alvarez, M. Mierzejewski, and E. Dagotto, Nat. Commun. **12**, 2955 (2021).
[21] T. Giamarchi, *Quantum Physics in One Dimension*, Vol. 121 (Clarendon Press, Oxford, UK, 2003).
[22] E. Berg, E. Fradkin, and S. A. Kivelson, Phys. Rev. Lett. **105**, 146403 (2010).
[23] G. Y. Cho, R. Soto-Garrido, and E. Fradkin, Phys. Rev. Lett. **113**, 256405 (2014).
[24] J. May-Mann, R. Levy, R. Soto-Garrido, G. Y. Cho, B. K. Clark, and E. Fradkin, Phys. Rev. B **101**, 165133 (2020).
[25] A. Tsvelik, Proc. Natl. Acad. Sci. USA **116**, 12729 (2019).
[26] A. Bohrdt, L. Homeier, I. Bloch, E. Demler, and F. Grusdt, arXiv:2108.04118.
[27] A. Bohrdt, L. Homeier, C. Reinmoser, E. Demler, and F. Grusdt, Ann. Phys. **435**, 168651 (2021).
[28] M. Y. Kagan, D. Khomskii, and M. Mostovoy, Eur. Phys. J. B **12**, 217 (1999).
[29] K. Kojima, A. Keren, L. Le, G. Luke, W. Wu, Y. Uemura, K. Kiyono, S. Miyasaka, H. Takagi, and S. Uchida, J. Magn. Magn. Mater. **140-144**, 1657 (1995).

[30] S. R. White, Phys. Rev. Lett. **69**, 2863 (1992).
[31] S. R. White, Phys. Rev. B **48**, 10345 (1993).
[32] I. P. McCulloch, arXiv:0804.2509.
[33] J. Hauschild and F. Pollmann, SciPost Phys. Lect. Notes 5 (2018).
[34] A. Jaefari and E. Fradkin, Phys. Rev. B **85**, 035104 (2012).
[35] A. M. Tsvelik, Phys. Rev. B **94**, 165114 (2016).
[36] F. Anfuso and A. Rosch, Phys. Rev. B **75**, 144420 (2007).
[37] R. Verresen, J. Bibo, and F. Pollmann, arXiv:2102.08967.
[38] S. Mishra, G. Catarina, F. Wu, R. Ortiz, D. Jacob, K. Eimre, J. Ma, C. A. Pignedoli, X. Feng, P. Ruffieux *et al.*, Nature (London) **598**, 287 (2021).
[39] G. Catarina and J. Fernández-Rossier, Phys. Rev. B **105**, L081116 (2022).
[40] M. Ogata, M. U. Luchini, S. Sorella, and F. F. Assaad, Phys. Rev. Lett. **66**, 2388 (1991).
[41] Note that $\eta_a\eta_b = \pm i$ because $(\eta_a\eta_b)^2 = 1$. In the end we only care about the correlation function of the spin operators, where a pair of $\eta_a\eta_b$ appear. Thus, whether $\eta_a\eta_b = i$ or $\eta_a\eta_b = -i$ does not matter. Here we make one choice just for simplicity.